

**INVESTIGATION OF CELLULOSE SEPARATOR  
IN ALUMINIUM-AIR BATTERY**

**Lye Jun Yan**

**UNIVERSITI TUNKU ABDUL RAHMAN**

**INVESTIGATION OF CELLULOSE SEPARATOR IN ALUMINIUM-  
BATTERY**

**Lye Jun Yan**

**A project report submitted in partial fulfilment of the  
requirements for the award of Bachelor of Mechanical  
Engineering with Honours**

**Lee Kong Chian Faculty of Engineering and Science  
Universiti Tunku Abdul Rahman**

**April 2024**

**DECLARATION**

I hereby declare that this project report is based on my original work except for citations and quotations which have been duly acknowledged. I also declare that it has not been previously and concurrently submitted for any other degree or award at UTAR or other institutions.

Signature : Lye

Name : Lye Jun Yan

ID No. : 2000992

Date : 29 April 2024

**APPROVAL FOR SUBMISSION**

I certify that this project report entitled **“INVESTIGATION OF CELLULOSE SEPARATOR IN ALUMINIUM-BATTERY”** was prepared by **LYE JUN YAN** has met the required standard for submission in partial fulfilment of the requirements for the award of Bachelor of Mechanical Engineering with Honours at Universiti Tunku Abdul Rahman.

Approved by,

Signature : *WengCheong*  
\_\_\_\_\_

Supervisor : Tan Weng Cheong  
\_\_\_\_\_

Date : 29 April 2024  
\_\_\_\_\_

Signature : \_\_\_\_\_

Co-Supervisor : \_\_\_\_\_

Date : \_\_\_\_\_

The copyright of this report belongs to the author under the terms of the copyright Act 1987 as qualified by Intellectual Property Policy of Universiti Tunku Abdul Rahman. Due acknowledgement shall always be made of the use of any material contained in, or derived from, this report.

© 2024, Lye Jun Yan. All right reserved.

## **ACKNOWLEDGEMENTS**

I would like to thank everyone who had contributed to the successful completion of this project. I would like to express my gratitude to my research supervisor, Dr. Tan Weng Cheong for his invaluable advice, guidance and his enormous patience throughout the development of the research.

## ABSTRACT

In the face of escalating energy demands and the imperative shift towards sustainable energy sources, batteries play a pivotal role in enabling this transition. Among the array of battery technologies, aluminum-air batteries stand out for their high energy density, cost-effectiveness, and abundance of aluminum resources. This study investigates the feasibility of utilizing cellulose-based separators which is fabricated by conifer cellulose in aluminum-air coin cell batteries, addressing key challenges such as separator degradation and electrolyte byproduct formation. Through meticulous experimentation, various cellulose separators with different binders, weight ratios and total mass were evaluated for their performance. Results revealed significant variations in discharge behavior and peak power output based on binder type, weight ratio, and total mass by using both discharge and linear sweep voltammetry (LSV) test. Separator with carboxymethyl cellulose (CMC) binders produced shorter discharge periods and lower plateau voltages than polyvinyl alcohol (PVA) binders. Doubling overall mass while retaining the same weight ratio significantly enhanced performance, especially with carboxymethyl cellulose (CMC) binders, resulting in longer discharge times and higher peak outputs. The best-performing separator had 75% nanofibrils cellulose (CNF) and 25% carboxymethyl cellulose (CMC) by weight, for a total mass of 0.6g. This separator discharged in 1121 seconds with a discharge current of 20mA and a plateau voltage of 1.15V during the discharge test. In the LSV test, it achieved a peak power of 47.8mW. Therefore, the CNF75CMC25 separator weighing 0.6g was then used in an aluminum coin cell battery, resulting in a discharge time of 160 seconds, a plateau voltage of 1.15V, and a peak power of 12.4mW.

## TABLE OF CONTENTS

<b>DECLARATION</b>	<b>i</b>
<b>APPROVAL FOR SUBMISSION</b>	<b>ii</b>
<b>ACKNOWLEDGEMENTS</b>	<b>iv</b>
<b>ABSTRACT</b>	<b>v</b>
<b>TABLE OF CONTENTS</b>	<b>vi</b>
<b>LIST OF TABLES</b>	<b>viii</b>
<b>LIST OF FIGURES</b>	<b>ix</b>
<b>LIST OF SYMBOLS / ABBREVIATIONS</b>	<b>x</b>

### CHAPTER

<b>1</b>	<b>INTRODUCTION</b>	<b>1</b>
	1.1 General Introduction	1
	1.2 Importance of the Study	2
	1.3 Problem Statement	2
	1.4 Aim and Objectives	3
	1.5 Scope and Limitation of the Study	3
	1.6 Contribution of the Study	4
	1.7 Outline of the Report	4
<b>2</b>	<b>LITERATURE REVIEW</b>	<b>6</b>
	2.1 Introduction	6
	2.2 Anode	7
	2.2.1 Pure Aluminium	8
	2.2.2 Aluminium Alloy	9
	2.3 Separator	12
	2.4 Air cathode	15
	2.5 Electrolyte	19
	2.5.1 Aqueous Electrolyte	19
	2.5.2 Non-Aqueous Electrolyte	21



2.6	Summary	24
<b>3</b>	<b>METHODOLOGY AND WORK PLAN</b>	<b>25</b>
3.1	Introduction	25
3.2	Material Preparation	25
3.3	Overall Design of Battery	26
3.4	Preparation of Electrolyte	27
3.5	Preparation of Aluminium Anode	27
3.6	Preparation of Air Cathode	27
3.7	Preparation of Separator	27
3.8	Testing	28
<b>4</b>	<b>RESULTS AND DISCUSSION</b>	<b>29</b>
4.1	Introduction	29
4.2	Performance of the separators	29
4.2.1	Cellulose separators with PVA binder	29
4.2.2	Cellulose separators with CMC binder	33
4.3	Cellulose Separators with Doubled Total Mass Utilizing CMC or PVA Binders	35
4.4	Coin Cell Battery Characterization	41
<b>5</b>	<b>CONCLUSION AND RECOMMENDATION</b>	<b>44</b>
5.1	Conclusion	44
5.2	Recommendation	44
	<b>References</b>	<b>46</b>

**LIST OF TABLES**

Table 2.1: Energy Densities of Different Metal Air Batteries(Mori, 2020)	7
Table 4.1: Separator Composition and Corresponding Masses	30
Table 4.2: Comparison Table of Separators Utilizing PVA Binder	30
Table 4.3: Separator Composition and Corresponding Masses(CMC binder)	33
Table 4.4: Comparison Table of Separators Utilizing CMC Binder	33
Table 4.5: Separator Composition and Corresponding Masses (PVA binder)	36
Table 4.6: Separator Composition and Corresponding Masses(CMC binder)	36
Table 4.7: Comparison Table of Doubled Separator Masses Separators Utilizing different binders.	36

**LIST OF FIGURES**

Figure 3.1: Work Plan Flowchart	25
Figure 3.2: Overall design of aluminium-air battery.	26
Figure 3.3: Overall Assembly Process of the coin cell battery.	26
Figure 4.1: Discharge Curve with Varied Separator Weight Ratios with PVA binder	30
Figure 4.2: LSV Curve with Varied Separator Weight Ratios	31
Figure 4.3: Discharge Curve with Varied Separator Weight Ratios with CMC binder	34
Figure 4.4: LSV Curve with Varied Separator Weight Ratios with CMC binder	34
Figure 4.5: Discharge Curve with Doubled Separator Masses and Varied Weight Ratios of both PVA and CMC Binders	37
Figure 4.6: LSV Curve with Doubled Separator Masses and Varied Weight Ratios of both PVA and CMC Binders	37
Figure 4.7: Discharge Curves for CNF75CMC25 Separator with Varied Total Mass	40
Figure 4.8: LSV Curves for CNF75CMC25 Separator with Varied Total Mass	40
Figure 4.9: Discharge Curve of Coin Cell Battery Utilizing Optimal Separator Composition	41
Figure 4.10: LSV Curve of Coin Cell Battery Utilizing Optimal Separator Composition	42

**LIST OF SYMBOLS / ABBREVIATIONS**

AAB	Aluminium-Air battery
OOR	Oxygen Reduction Reaction
AC	Activated Carbon
CB	Carbon Black
$MnO_2$	Manganese Dioxide
PTFE	Polytetrafluoroethylene
CMC	Carboxymethyl Cellulose
PVA	Polyvinyl Alcohol
KC	Kappa Carrageenan
CNF	Nanofibrils Cellulose

## CHAPTER 1

### INTRODUCTION

#### 1.1 General Introduction

In this era of rapid industrial development, coupled with a high population growth rate and limited access to non-renewable energy sources, the world is experiencing an escalating energy crisis due to the high demand for energy. Energy storage devices are vital in facilitating the transition to the usage of clean and sustainable energy for the future. Therefore, it is imperative to study the battery as one of the energy storage devices commonly used in our daily lives. A battery is an energy storage system that consists of two electrodes (anode and cathode) immersed in an electrolyte solution, enabling an electrochemical reaction. The mechanism of a battery involves the flow of electrons from the anode to the cathode to provide energy during discharge, and the direction of electron flow is reversed during recharging. Batteries offer several advantages such as high energy density and suitable for various sectors such as electronic devices and electric vehicles. However, there are some limitations such as a relatively short lifespan and slower charging times compared to other energy storage systems.

Currently, metal-air batteries, especially aluminium-air batteries, are under extensive investigation across various aspects to enhance their practical applicability. Ryu et al. (2019) have summarized several factors, including a high volumetric capacity of approximately  $8040 \text{ Ah L}^{-1}$ , lower cost, and the abundance of aluminium compared to other metals like zinc and lithium (Ryu, Park and Cho, 2019). Moreover, Ryu et al. have also highlighted the advantages of aluminium-air batteries, such as a smaller overall size due to the utilization of ambient air and a theoretical energy density of  $8100 \text{ Wh kg}^{-1}$  (Ryu, Park and Cho, 2019). In addition to this, Mutlu and Yazıcı have noted the superiority of aluminium-air batteries in electric vehicles (EVs), with up to a 15-fold increase in performance compared to lead-acid batteries, while simultaneously reducing weight due to their lightweight characteristics (Mutlu and Yazıcı, 2019). Therefore, there is a high likelihood of substituting lithium-ion batteries with

aluminium-air batteries due to the drawbacks of lithium-ion batteries, including cost and safety concerns. (Manthiram, 2011)(Li et al., 2009). In this study, the performance and potential applications of the aluminum-air battery within a coin cell will be further investigated to offer a efficient energy storage solution.

## **1.2 Importance of the Study**

This study covers a wide range of topics, such as battery production methods, electrode designs and its implications go far beyond aluminium-air batteries. The findings of these investigations may have an impact on the development of additional battery technologies, potentially leading to disruptive discoveries in the overall energy storage field. Furthermore, the high energy density of aluminum-air batteries is a significant advantage, especially when implemented in a small size. These batteries solve concerns about shortages of resources and geopolitical dependencies associated with batteries that rely on rare metals like lithium or cobalt by utilizing abundant and non-scarce materials like aluminium. Moreover, the usage of aluminium-air battery can dramatically cut greenhouse gas emissions pushing technological innovation and significantly contributing to a cleaner, greener, and more sustainable future.

## **1.3 Problem Statement**

Although aluminium-air batteries exhibit greater potential for future practical applications, there will have certain issues for instance the byproduct will affect the air cathode (Mori, 2020). Mutlu and Yazıcı have highlighted one of the significant drawback for aluminium-air battery which is the fast degradation of the anode due to the corrosion behaviour of aluminium with electrolyte and the release of the hydrogen gas which might causing the by-product deposit on the surface of the anode preventing the electrochemical reaction (Mutlu and Yazıcı, 2019). Apart from that, Palanisamy et al. have stated that anode with a pure aluminium material will result in passivation of the surface of Al due to the by-product of side reaction and affect the overall performance. (Palanisamy et al., 2021).

Apart from that, the selection and optimization of appropriate separator materials for aluminium-air batteries represents a major problem. The separator

is essential in preventing direct contact and unwanted reactions between the cathode and anode. However, the impact of different separator materials, types, and ratios on overall battery performance requires further study to fully understand their relationships. Therefore, comprehensive testing and research into various separator materials are essential to identify optimal alternatives that deliver superior battery performance while remaining cost-effective.

#### **1.4 Aim and Objectives**

The aim of the study is to investigate the feasibility of using cellulose-based separator in a coin cell aluminium-air battery. There are three objectives required to be achieved in this study:

- (i) To prepare a cellulose-based separator for aluminium-air battery.
- (ii) To investigate the electrical performance of an aluminium-air battery.
- (iii) To fabricate an aluminium coin cell battery.

#### **1.5 Scope and Limitation of the Study**

The scope of the study on the fabrication of aluminum coin cell batteries encompasses various critical aspects of this emerging energy storage technology. The research will primarily focus on developing an anode using an aluminum plate, employing a potassium hydroxide electrolyte with an ethyl-acetate additive, and fabricating an air cathode using nickel mesh, activated carbon (AC), carbon black (CB), manganese dioxide ( $\text{MnO}_2$ ), polytetrafluoroethylene (PTFE), and propanol. There are two different types of separators in this study, including carboxymethyl cellulose (CMC) with a polyvinyl alcohol (PVA) binder and nanofibrils cellulose (CNF) with a PVA binder. Furthermore, the study will conduct a thorough performance analysis to evaluate the capabilities of the fabricated batteries.

However, there are several inherent limitations to this study that must be addressed. First and foremost, the performance analysis parameters may be limited due to the availability of laboratory facilities and equipment. Furthermore, there are only two types of separators to be compared, and this limitation may reduce the comprehensiveness of the performance study due to the insufficient data that can be collected.

## **1.6 Contribution of the Study**

The study greatly contributes to the improvement of cellulose-based separators and battery technology by conducting a thorough examination of several separator topologies. The best separator composition was determined through systematic testing of various binders, weight ratios, and total masses, resulting in greater performance in terms of discharge duration, plateau voltage, and peak power. This understanding of the relationship between binder type, concentration, and battery performance can help designers create cellulose separators with improved mechanical strength, stability, and ion transport qualities. Additionally, the use of cellulose, a biodegradable and renewable resource, offers significant advantages in combating environmental problems by reducing reliance on synthetic, non-biodegradable materials and lowering the environmental impact of battery production and disposal.

## **1.7 Outline of the Report**

Chapter 2 is a comprehensive literature analysis that focuses on the importance of separators in batteries. It explores each component of a battery, including the cathode, anode, electrolyte, and separator, emphasizing the importance of separators in improving battery performance and safety. The chapter also examines current materials and technology utilized in battery separators, with a particular emphasis on cellulose-based separators. This chapter provides valuable insights into the present state of field research by combining literature findings.

Chapter 3 describes the methodology used in the experimental investigation. It outlines the materials and equipment used in the construction of cellulose-based separators, as well as the experimental setup and circumstances. The chapter also discusses the parameters examined and their significance, as well as the data gathering methods and quality control mechanisms used.

Chapter 4 summarizes the results of the experimental study and begins a discussion of the findings. The chapter opens with the reporting of experimental data, which include the characterization of cellulose-based



separators and their performance evaluation in terms of ion conductivity, mechanical strength, and temperature stability. It then discusses the implications of these findings in regard to the study aims, comparing them to existing literature and examining any limitations or sources of error discovered during the experiment. Finally, the chapter discusses the results' broader implications for battery technology and recommends potential areas for future research.

Chapter 5 summarizes major findings, reiterates research aims, and emphasizes the study's significance to the field. The study's practical ramifications and uses are examined, along with recommendations for future research or development.

## CHAPTER 2

### LITERATURE REVIEW

#### 2.1 Introduction

There has been a noticeable increase in research on metal-air batteries because non-renewable energy sources are becoming more difficult to obtain and because it is important to promote global sustainability. Currently, lithium-ion batteries are extensively employed worldwide due to their matured technology that allows the production of secondary batteries across various sizes. Nevertheless, the expense of lithium-ion batteries remains a noteworthy factor, closely linked to the cost of essential raw materials like electrodes, separators, and electrolytes used in the battery's components (Mori, 2020). Furthermore, addressing the lifespan of lithium-ion batteries presents a significant challenge as their maximum efficiency degrades rapidly over time even during periods of non-use. (Ahuja et al., 2021) Additionally, the energy density of existing lithium-ion batteries at approximately 160-180 Wh/kg is inadequate for ensuring their long-term durability in today's technology landscape, particularly in light of the ambitious goal to replace all conventional vehicles with electric cars. (Chen et al., 2022)

Numerous studies suggest that metal-air batteries are emerging as viable alternatives due to their superior energy density and environmentally sustainable attributes when compared to prevalent battery technologies like lithium-ion and lead-acid batteries. The fundamental principle behind metal-air batteries involves the fusion of a metal anode with an air-based cathode, resulting in diverse reactions based on the choice of metal. Varieties of metals such as lithium, aluminium, and zinc exhibit distinct reaction mechanisms within this battery system. (Lee et al., 2010) According to the table 2.1 that are concluded by Mori, lithium-air batteries show the highest theoretical specific energy 5210 Wh/kg among all the metal-air batteries. (Mori, 2020)

Table 2.1: Energy Densities of Different Metal Air Batteries(Mori, 2020)

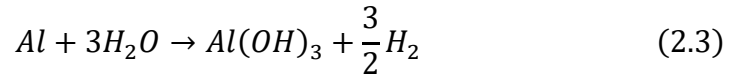
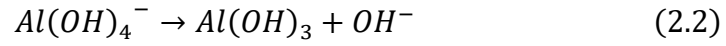
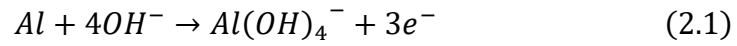
Metal air battery	Theoretical specific energy Wh kg <sup>-1</sup> (including oxygen)	Theoretical specific energy Wh kg <sup>-1</sup> (excluding oxygen)	Calculated open circuit voltage (V)
Calcium-air	2990	4180	3.12
Germanium-air	1480	7850	1.00
Iron-air	1431	2044	1.30
Aluminium-air	4300	8140	1.20
Lithium-air	5210	11140	2.91
Sodium-air	1677	2260	2.30
Magnesium-air	2789	6462	2.93
Potassium-air	935	1700	2.48
Zinc-air	1090	1350	1.65
Tin-air at 1000 K	860	6250	0.95

In this chapter, literature review is performed to understand the topics that are required and relevant in this study. The main focuses of this chapter are on the components of the aluminium coin cell battery including both electrodes, anode and cathode, electrolyte and separator.

## 2.2 Anode

Extensive research has been dedicated to investigating aluminium (Al) anodes in Al-air batteries, given their crucial role in determining battery performance. An aluminium anode is considered a promising candidate due to its advantageous characteristics, including a high theoretical energy capacity of 2.90 Ah/g, compared to lithium's 3.86 Ah/g, and a low atomic weight of 26.98 (Li and Bjerrum, 2002). However, when aluminium electrodes participate in the reaction outlined in equation (2.1) within an alkaline electrolyte, it results in the production of aluminium hydroxide precipitates. Simultaneously, equation (2.2) shows that an oxide layer forms and envelops the electrode's surface, leading to an increase in internal resistance. This delay in achieving a consistent voltage state can thus have a significant effect on the battery's performance. Additionally, a parasitic corrosion reaction, as shown in equation (2.3), limits the consumption of metal and the release of hydrogen gas (Ding et al., 2016). The parasitic hydrogen evolving effect and the bubble shielding effect will cause a dominant loss of kinetic in the aqueous aluminium-air battery compared to ohmic loss and mass transfer loss (Zhou, Bhonge and Cho, 2020). Therefore, in

this section will provide insights into the impacts of both pure aluminium anodes and alloyed aluminium anodes on the electrochemical behaviour on battery.



### 2.2.1 Pure Aluminium

There is a significant amount of research focused on evaluating battery performance when utilizing pure aluminum as the anode. Mori's statement implies that improving the electrochemical performance of a battery entails substituting impure aluminum anodes with pure aluminum (Mori, 2020). According to Palanisamy et al., the electrochemical properties by utilizing pure Al as anode results in excellent electrochemical properties. (Palanisamy et al., 2021).

Cho et al. contributed valuable insights to the examination of battery performance using two distinct grades of aluminium: 2N5 (99.5 % purity) and 4N (99.99 % purity) in a 4 M NaOH electrolyte. As a result, it was found that the battery performance of 2N5 grade aluminium is lower compared to that of 4N grade aluminium at standby and low-power discharge levels. This discrepancy arises because 2N5 grade aluminium forms a complex film containing impurities like Fe and Si, resulting in a reduction in standby battery voltage. Reducing the discharge voltage from 1.0 V to 0.8 V has the potential to significantly enhance battery efficiency, with an estimated improvement of approximately 21.03% for 4N aluminium and approximately 57 % for 2N5 aluminium. Furthermore, the researchers also discovered that the complex film on 2N5 grade aluminium dissipates at higher power discharge rates, leading to a convergence in discharge current densities between 2N5 and 4N grade aluminium. (Cho et al., 2015).

In a further study conducted by Peng, G.S. et al., the focus was on the utilization of three distinct purity grades of aluminium anodes: 2N (99.95 % Al), 4N (99.99 % Al), and 5N (99.999 % Al) to investigate both the discharge and self-corrosion behaviors of these anodes in an alkaline solution. The results unveiled a clear trend in self-corrosion rates, with 5N Al displaying the lowest rate, followed by 4N Al, and then 2N Al. This reduction in self-corrosion rates was attributed to the presence of impurity particles containing iron (Fe), which had a significant impact. Furthermore, the discharge behavior of aluminium anodes was examined at both low (10 mA/cm<sup>2</sup>) and high (100 mA/cm<sup>2</sup>) constant current densities. The results demonstrated that the 4N Al anode consistently exhibited the highest operating voltage, measuring 1.18 V at low current densities and 0.48 V at high current densities. Therefore, higher aluminium purity corresponded to decreased resistance to self-corrosion but increased electrochemical activity (Peng et al., 2020).

### **2.2.2 Aluminium Alloy**

Currently, the high self-corrosion rate of aluminium anodes is a significant challenge that limits their practical use. To address this issue, researchers are increasingly investigating the incorporation of different elements into aluminium electrodes. It has been recognized that doping aluminium with various elements is the most promising and effective approach for enhancing its electrochemical properties (Zhou, Bhonge and Cho, 2020). ZHUANG et al. also stated that the addition of trace alloying elements to aluminium anode materials can significantly diminish the problem of low current which caused by self-corrosion and improving discharge performance (ZHUANG et al., 2021). Moreover, Abedin & Endres have reported that the problem of passivation for aluminium can be solved by choosing suitable alloying elements such as Sn, Zn and so on (Zein El Abedin and Endres, 2004).

El Abedin & Saleh have developed several aluminium alloys and each alloyed with distinct elements such as Ga, In, Pb, Cd, Hg, Sn, and Zn. These alloys are utilized as anodes in alkaline batteries to assess their efficacy within battery systems. The findings reveal that both Al-In and Al-Mn exhibit high self-corrosion rates indicating their unsuitability for application as anodes. On

the contrary, Al-Ga-In demonstrates good performance in terms of self-corrosion rate and exhibits the largest negative open circuit potential due to the presence of In causes the oxidizing layer to be destroyed. Furthermore, Al-In-Ga alloy gives an anode efficiency of 92 %. Taking all these factors into account within the scope of this experiment, Al-Ga-In demonstrate an effective anode such as highly negative open circuit potential(-1610 mV), minimal self-corrosion ( $0.43 \text{ mg cm}^{-2} \text{ min}^{-1}$ ) and strong anode efficiency (92 %) (Zein, Abedin and Saleh, 2004).

Furthermore, Tang et al. studied the battery performance and efficiency with the interaction between zinc and the aluminium anode. Literature reveals that the introduction of zinc and indium as an alloying element Al-In-Zn can potentially decrease the resistance and improve the electrode under high-rate current. Furthermore, the self-corrosive potential of Al-In-Zn alloys is at -1.64 V which is 70 mV lower than pure aluminium in NaOH( $4 \text{ mol L}^{-1}$ ). Other than that, the experiment experimental results indicate that the activation potential of electrode is shifted to more negative values and also helps in decreasing the hydrogen evolution effectively as  $\text{Zn}(\text{OH})_2$  covers the surface of the electrode in the process of polarization by adding  $\text{Zn}^{2+}$  to the Al-In alloys in aqueous NaCl. Consequently, the additive of zinc on the aluminium anode in the aluminium-air battery lower the anodic polarization, decrease production of hydrogen and shift the electrode potential to negative values(Tang et al., 2004).

Ren et al. investigated the impact of alloying aluminium with magnesium and tin is compared to pure aluminium (Al) to assess their suitability as anodes for aluminium-air batteries in a  $4 \text{ mol L}^{-1}$  KOH solution. The experiment demonstrated that the alloyed aluminium anodes outperformed pure aluminium in terms of corrosion resistance. Specifically, the self-corrosion for pure aluminium exhibited at a rate of  $10.86 \text{ mg.cm}^{-2} \text{ h}^{-1}$  whereas Al-Sn showed a rate of  $5.78 \text{ mg.cm}^{-2} \text{ h}^{-1}$ , Al-Mg had a rate of  $1.25 \text{ mg.cm}^{-2} \text{ h}^{-1}$  and Al-Mg-Sn recorded a rate of  $3.06 \text{ mg.cm}^{-2} \text{ h}^{-1}$ . Notably, Al-Mg alloy displayed the lowest self-corrosion rate and the highest capacity among the tested alloys, while Al-Mg-Sn demonstrated superior

electrochemical performance and battery discharge capabilities. The results of this study emphasize the potential of alloyed aluminium anodes, in particular Al-Mg-Sn to improve the efficiency of aluminium-air batteries by providing better corrosion resistance and increased capacity for energy storage. (Ren et al., 2019)

Apart from alloying aluminium with other elements, the activation aluminium can be done by introducing small amounts of appropriate metal cations like  $In^{3+}$ ,  $Ga^{3+}$ ,  $Hg^{2+}$ ,  $Sn^{4+}$ , and  $Sn^{2+}$  into the electrolyte. (El Abedin & Saleh, 2004). Abedin & Endres have reported that the addition of  $Zn^{2+}$  ions can significantly activate the aluminium in 0.6M NaCl solution by studying the behaviour of aluminium (Al), Al-In, and Al-Ga-In alloys when exposed to chloride solutions. Al-In alloy exhibited the most negative open circuit potential in a 0.6 M NaCl solution with lowest corrosion resistance compared to Al and Al-Ga-In. Secondly, the initial dissolution of the Al-In electrode led to an increase in  $In^{3+}$  ion concentration in the electrolyte, subsequently causing redeposition of In at active sites on the electrode surface and facilitating  $Cl^-$  adsorption at highly negative potentials. Thirdly, in the presence of  $Zn^{2+}$  in the electrolyte, potentiostatic I/t results showed minimal impact on the Al electrode. Lastly, the addition of  $Zn^{2+}$  had negligible effects on the polarization resistance of Al, but for Al-In and Al-Ga-In, it led to reduced polarization resistance, indicating the activating influence of  $Zn^{2+}$  ions. (Abedin & Endres, 2004)

Shayeb et al. also explored how  $In^{3+}$  ions affect the activation of aluminium in different alloys such as Al, Al-Sn, Al-Zn, and Al-Zn-Sn. The result shows that the addition of  $In^{3+}$  ions led to the activation of pure Al, Al-Zn, and Al-Zn-Sn electrodes and this activation increased as the concentration of  $In^{3+}$  ions increased. Moreover,  $In^{3+}$  had a stronger activating effect on the Al-Zn alloy compared to pure Al due to the formation of  $ZnAl_2O_4$  spinel, resulting in increased defects in the protective layer. Conversely, the activating effect of  $In^{3+}$  was diminished in Al-Zn-Sn alloy compared to the Al-Zn alloy. In the Al-Sn alloy, the presence of Sn hindered the diffusion of In into the alloy, along with the presence of iron impurities, leading to deactivation. In summary,

the activation mechanisms of pure Al, Al-Zn, and Al-Zn-Sn appeared to be similar, contingent on the availability of defect sites and the deposition of In at these sites (Shayeb et al., 1999).

### 2.3 Separator

The separator plays a vital role in liquid electrolyte batteries other than electrodes and electrolyte as it separates electrodes to avoid contacting each other while facilitating the movement of ions. There are several factors of separator membrane including chemical and electrochemical stability, thickness, porosity, pore size, permeability, mechanical strength, wettability, dimensional stability, thermal shrinkage, shutdown and also cost need to be considered to fabricate a suitable separator (Zhang, 2007).

Jana et al. have summarized several types of separators and each of them will have different properties which will significantly affect the performance of battery. Firstly, the microporous separator is defined as a separator within a pore diameter of 5-10 nm which is fabricated using organic polymers such as polyethylene, polypropylene, poly(vinyl chloride) and poly(tetrafluoroethylene). They are usually made by two ways including wet process and dry process. Another type of the separator is nonwoven mat separators which are defined as a separator within a thickness about 100-200  $\mu\text{m}$  and the common way to fabricate them including electrospinning and melt-blowing. The third type of the separator is polymer electrolyte membranes which will be classified into solid and liquid electrolyte membranes. Lastly is the composite membrane separator which is introduced to solve the problem of a conventional separator by introducing an coating layer to improve the properties of the separator like thermal resistance, wettability and so on (Jana et al., 2018).

Nowadays, polyolefin-based microporous separators which is made of PE, PP, other polyolefins have been widely used in the Li-ion separator market due to their properties like thickness, impressive chemical resistance and excellent mechanical characteristics (Huang, 2011). There are also some of the research prove that the performance of the polyolefin-based microporous separators can be enhanced by modify the surface without changing the



thickness. For example, Zhao et al. have studied the thermal stability of polyolefin separators within lithium-ion batteries by introducing surface chemical modifications to enhance battery energy density. The remarkable outcome was a significant reduction in thermal shrinkage, from 38.6% in pristine separators to a mere 4.6 % in the modified ones after exposure to 150 °C for 30 minutes. Moreover, the modified separators maintained similar thicknesses to the original ones. Electrochemical tests demonstrated that lithium-ion battery half-cells employing these modified separators exhibited nearly indistinguishable performance compared to those using commercially coated separators with silica nanoparticles (Zhao et al., 2015).

Then, Tan, W.C. *et al.* have done research on evaluating the discharge behaviour of aluminium-air battery by implementing the polypropylene separator into it. They fabricated two different separators: a polypropylene separator and a paper-based separator constructed from Kimwipes with a 1M KOH electrolyte under a range of discharge currents. The results clearly preferred the polypropylene separator as it demonstrated a significant threefold improvement in discharge duration at 10 mA, lasting nearly 97 minutes compared to Kimwipes' paltry 33 minutes. Furthermore, polypropylene demonstrated superior voltage stability with a steady voltage reduction after an initial dip from 1.1 V to 0.9 V, whereas Kimwipes experienced rapid voltage drops from 1.18 V to 0.82 V. The paper-based separator took approximately 28 minutes to fully discharge at a 20mA rate, which was less than that of the polypropylene-based aluminium-air battery, which was 52 minutes. Even at higher discharge currents 30mA, polypropylene consistently outperformed Kimwipes, demonstrating more stable voltage output and longer discharge durations (Tan et al., 2021) .

However, it's important to note that polyolefin separators typically exhibit limited thermal stability. They undergo considerable shrinkage within the temperature range of 90–120 °C and reach their melting point at temperatures between 150–200 °C, with the exact melting point depending on the specific polymer used (Huang, 2011). Apart from that, none of polyolefin separators can withstand temperatures around 165 °C and might lead to

dangerous direct contact between electrodes, triggering hazardous chemical reactions (Zhang, 2007). Therefore, more and more research are focusing on cellulose-based composite separator as they have good electrolyte wettability, high ionic conductivity, excellent flame retardancy and superior thermal resistance which improving the safety characteristics of battery (Zhang et al., 2014).

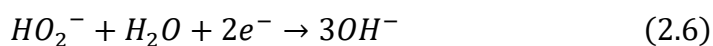
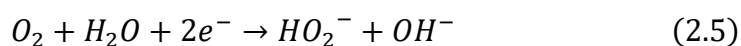
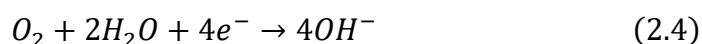
Lalia et al. investigated how the nanocrystalline cellulose NCC content influenced properties such as tensile modulus, thermal behaviour, and the thermal characteristics of the resulting nanocomposite films. Nanocrystalline cellulose (NCC) was produced by using acid hydrolysis method applied to Kim Wipes tissue papers. Subsequently, NCC was integrated into nanocomposite films composed of poly (vinylidene fluoride-co-hexafluoropropylene) (PH) using an electrospinning technique, with varying concentrations of NCC in the PH matrix. Notably, the most favourable composition was identified as PH with 2 wt % NCC, resulting in a substantial 75% enhancement in tensile modulus. Dynamic mechanical analysis of this PH nanocomposite containing 2 wt % NCC showcased elevated tensile modulus values between temperature of 30 to 150 °C (Lalia, Samad and Hashaiekh, 2012).

Other than that, Selan et al. also evaluated the performance of aluminium-air battery separators made from two different ratios of water hyacinth cellulose nanofibrils (WHCNF) and polyethylene glycol binder (PEG400), alongside a conventional filter paper separator through constant current discharge testing at 10 mA. Specifically, separators with compositions of 85 wt% WHCNF to 15 wt% PEG400 (WHCNF85:PEG15) and 65 wt% WHCNF to 35 wt% PEG400 (WHCNF65:PEG35) are prepared for the experiment. The result shows that the water hyacinth cellulose-based separators outperformed the filter paper separator, demonstrating superior initial voltages and extended discharge durations. WHCNF85:PEG15 and WHCNF65:PEG35 separators exhibited initial voltages of 1.00 V and 1.02 V, coupled with discharge times of 290.52 min and 323.68 min respectively whereas the filter paper separator yielded 0.4 V and 38.75 min. Furthermore, these cellulose separators generated peak power outputs of 10.04 mW/cm<sup>2</sup> and 10.81 mW/cm<sup>2</sup>,

surpassing the performance of a sodium chloride-based battery (Selan et al., 2023).

## 2.4 Air cathode

Air cathode is one of the electrodes that the reaction of oxygen molecules take place to gain the electrons. Generally, there are three components to form an air cathode including a current collector, a gas diffusion layer and a catalyst. It is an important component as the performance of Al-air batteries are significantly affected by air-cathode catalytic materials so it must be optimized (Mori, 2020). Currently, the widespread use of Al-air batteries faces a significant challenge due to the slow-paced oxygen reduction reaction (ORR) occurring at the cathode (Goel, Dobhal and Sharma, 2020). Furthermore, in the case of rechargeable or secondary metal-air batteries, performance limitations arise from both the catalytic oxygen reduction reaction (ORR) taking place during the discharging process and the oxygen evolution reaction (OER) occurring during the charging process. (Zhang et al., 2019). Based on the comprehensive review of Liu et al., the oxygen reduction reaction (ORR) will undergo in two paths in alkaline medium. One of the preferred pathways is shown in equation (2.4) which is called as a direct four-electron pathway and another is expressed by equation (2.5), (2.6) and (2.7) which indicate the successive two-electron pathway (Liu et al., 2017). Liu et al. have also stated that the sluggish oxygen reactions and oxygen evolution reaction problem will limit the efficiency of the battery in discharging or recharging, resulting in a poor performance on energy and power density of battery (Liu et al., 2021). Therefore, there is a critical need for a highly efficient catalyst that can expedite both ORR and OER reactions at the cathode, enabling the full realization of their potential. (Zhang et al., 2019)





Zhang et al. have provided one of the ways to enhance ORR efficiency is by integrating the electrocatalyst into the air cathode as it aids in maximizing battery performance. Therefore, investigating a suitable electrocatalyst is a crucial aspect that merits further exploration (Zhang et al., 2019). Nowadays Pt/C is one of the significant ORR electrocatalyst but accompany with some cons including its reserve scarcity and high cost affect the large-scale commercial application. Therefore, one of the solution is to develop low cost efficiency non-noble metal catalysts for aluminium-air battery (Cheng et al., 2021). Cheng et al. have created carbon nanofibers loaded with manganese oxides ( $MnO/Mn_2O_3/ONCNF-n$ ) which were doped with both oxygen and nitrogen to be served as catalysts for the oxygen reduction reaction (ORR) in alkaline environments. The result shows that  $MnO/Mn_2O_3/ONCNF-3$  catalysts exhibited excellent ORR performance and achieving an maximum power density of  $129.7 \text{ mW cm}^{-2}$  when they were applied in an aluminium-air battery (AAB). Therefore, this study provides an alternative option for non-noble ORR electrocatalyst for battery (Cheng et al., 2021).

Liu et al. have produced  $CeO_2$ , a special ORR enhancer, into a  $Co_3O_4$  catalyst that was supported by ketjenblack (KB) to evaluate the performance of electrocatalysts for the oxygen reduction reaction (ORR) in Al-air batteries.  $Co_3O_4 - CeO_2/KB$  is produced straightforward two-step hydrothermal process to be used as an ORR catalyst for Al-air batteries. The result shows that the addition of  $CeO_2$  nanoparticles significantly boosted the ORR activity of  $Co_3O_4/KB$ , even surpassing the benchmark Pt/C catalyst in alkaline conditions. Furthermore,  $Co_3O_4 - CeO_2 /KB$  demonstrated excellent electrocatalytic performance and long-term stability. This catalyst enabled a more efficient four-electron ORR pathway due to the synergy between  $CeO_2$  and  $Co_3O_4$ . In practical tests, Al-air batteries using  $Co_3O_4 - CeO_2/KB$  as the cathode catalyst consistently achieved higher discharge voltages compared to those with  $CeO_2 /KB$  or  $Co_3O_4 /KB$ . With its remarkable performance and cost-

effectiveness,  $Co_3O_4 - CeO_2/KB$  presents itself as a compelling alternative to the expensive Pt/C catalyst for Al-air batteries (Liu et al., 2016).

Kuo et al. have investigated the composite electrode that can be used to boost the performance of batteries by enhancing the oxygen reduction reaction (ORR) in the air electrode. The composite electrode is made of the combination of different crystal forms of manganese dioxide ( $MnO_2$ ), specifically alpha( $\alpha$ ) and beta-  $MnO_2$  ( $\beta$ ) with the conducting polymer poly-(3,4-ethylenedioxythiophene) (PEDOT). The result shows that the a-  $MnO_2/10AA$  sample had a stronger ORR current, reaching  $15.52 mA/cm^2$  at 0.7 V, while the b-  $MnO_2/10AA$  sample had a slightly lower current of  $12.96 mA/cm^2$ . The study found that the choice of crystalline phase of  $MnO_2$  strongly influenced the half-cell polarization curve test. Additionally, by incorporating PEDOT onto  $MnO_2/10AA$  samples as composite cathode materials, a significant enhancement in the ORR current was clearly observed, reaching a value of  $30.91 mA/cm^2$  for the PEDOT/a-  $MnO_2/10AA$  sample. This indicates that PEDOT/a-  $MnO_2$  exhibited higher conductivity than PEDOT/b-  $MnO_2$ , which contributed to improved charge transfer. (Kuo et al., 2015).

Apart from that, noble metals including platinum (Pt), palladium (Pd), gold (Au) and silver (Ag) also can be acted as a catalyst as the unoccupied d-orbital of noble metals help in absorb reactant molecules (Goel, Dobhal and Sharma, 2020). Lei et al. have demonstrated the design and production of an Ag-Cu film catalyst through Pulsed Laser Deposition (PLD). The resulting Ag50Cu50 film showcases remarkable catalytic activity in facilitating the Oxygen Reduction Reaction (ORR). This alloying of silver (Ag) and copper (Cu) within these embedded nanoparticles synergistically enhances the ORR catalytic performance. When applied in constructing a zinc-air battery, the primary battery delivers an impressive power density of  $67 mW cm^{-2}$ . Furthermore, the subsequent rechargeable zinc-air battery demonstrates low charge-discharge voltage polarization (1.1 V at  $20 mA cm^{-2}$ ) and outstanding stability over 100 charge and discharge cycles when operated in a natural air environment. In summary, the rechargeable battery displayed

excellent cycling performance, boasting a round-trip efficiency of 52.3 % in a Zn-air cell (Lei et al., 2015).

Sun et al. have developed a highly effective catalyst for the oxygen reduction reaction (ORR) by combining silver nanoparticles (Ag) with manganese oxide ( $MnO_2$ ) using a unique plating method. When tested, the 50 %Ag-  $MnO_2$  composite catalyst, with an equal ratio of Ag to  $MnO_2$ , outperformed individual Ag or  $MnO_2$  catalysts in terms of ORR activity and stability. Remarkably, when incorporated into an aluminium-air battery, this composite catalyst achieved a peak power density of  $204\text{ mWcm}^{-2}$ , surpassing the performance of a battery using only Ag ( $167\text{ mWcm}^{-2}$ ). These findings suggest that Ag-  $MnO_2$  composites hold promise for enhancing the efficiency of aluminium-air batteries (Sun et al., 2016).

Besides, Mori, R. have studied the performance of aluminium-air batteries by using a metal-organic framework (MOF) material as the cathode. The investigation involved a comparison of two air cathode materials, aluminium terephthalate (AT) and aluminium terephthalate conductive carbon (ATCC), both of which are MOF-based against the conventional activated carbon (AC) within an ionic-liquid electrolyte, specifically 1-ethyl-3-methylimidazolium chloride. The results indicated that the electrical power output and cell capacity were lower than those achieved with AC when AT and ATCC were used as air cathode materials. However, the battery's cell capacity remained stable and did not decline over repeated electrochemical cycles. Additionally, the study revealed the absence of major byproducts like  $Al(OH)_3$  and  $Al_2O_3$  on the anode electrode and the interfacial cell impedance did not increase after extended electrochemical reactions (Mori, 2017a).

Mori, R. even developed the air cathode of rechargeable aluminium-air battery by using various materials, including active carbon, carbon alloy, perovskite oxide, aluminium terephthalate (a metal-organic framework), and non-oxide ceramics like TiN, TiC, and  $TiB_2$ , were investigated. Among these materials, perovskite oxide, TiN, and TiC demonstrated remarkable stability in

electrochemical reactions over extended periods. Particularly, TiC as an air cathode material not only exhibited stable long-term battery performance but also effectively suppressed the formation of detrimental byproducts such as  $Al(OH)_3$  and  $Al_2O_3$ , marking a significant breakthrough. This study also highlights the potential of materials like TiN and TiC in mitigating byproduct formation and enhancing the feasibility of practical rechargeable aluminium-air batteries (Mori, 2017b).

## **2.5 Electrolyte**

Electrolytes constitute a fundamental aspect of aluminium-air battery functionality, typically classified into two categories: aqueous and non-aqueous. As highlighted by Goel et al., the primary role of the electrolyte is to prevent electrical short circuits between the battery's two electrodes and to supply  $OH^-$  ions, essential for sustaining electrochemical reactions (Goel, Dobhal and Sharma, 2020). Therefore, the choice of electrolyte emerges as a pivotal determinant significantly impacting the overall performance of the battery. Furthermore, van Ree (2020) highlights that the introduction of specific additives into the electrolyte leads to the formation of a layer on the electrode surfaces, effectively guarding them against undesired solvent reduction or oxidation reactions. This strategic use of additives possesses the potential to greatly enhance the battery's longevity, energy storage capacity, and safety (van Ree, 2020).

### **2.5.1 Aqueous Electrolyte**

Aqueous electrolytes are preferred over organic liquids, polymers, inorganic solid-state materials, and ionic liquid electrolytes in battery systems due to their superior characteristic including ionic conductivity, better wettability, enhanced safety features, and environmentally friendly properties. (Chen et al., 2022). There are three various types of water-based aqueous electrolytes and each of them is classified by their pH values like acidic electrolytes (pH 2-7), neutral electrolytes (pH 7) and alkaline electrolytes (pH 7-13). Nowadays, the majority of Al-air batteries employ alkaline solutions especially potassium hydroxide (KOH) and sodium hydroxide (NaOH) as electrolytes (Mori, 2020). Other than that, the performance of battery by using neutral electrolytes and acidic

electrolyte in aluminium-air battery have been studied since early. However, according to the Goel et al. stated that the performance of neutral electrolyte is lower when compared to alkaline electrolyte due to strong passivation on the anode. Therefore, when using a neutral electrolyte, the overall energy density of the battery is approximately one third compared to that achieved with alkaline electrolytes. (Goel, Dobhal and Sharma, 2020). This is because Farsak & Kardaş have explained that the alkaline electrolyte solution is commonly used as dissolving oxides always formed on the electrode surface when using neutral electrolyte which is a serious problem for the aluminium-air battery and can be avoided by using alkaline electrolyte. (Farsak and Kardaş, 2018) .

For example, Fan et al. have reported that the UFG Al anode with finer grain sizes exhibited improved battery performance in alkaline electrolyte due to the active dissolution of the Al anode. However, in the presence of NaCl electrolyte, the performance of fine grain size Al anode did not improved significantly as the blockage of the oxide film and local corrosion. Moreover, this research demonstrates that the fabrication of UFG Al anodes can enhance their performance in alkaline environments, making them a promising candidate for Al-air batteries. Notably, the use of 4 M NaOH as an electrolyte with the UFG Al anode appeared to be a preferable option as it exhibited lower polarization and promising energy density. Therefore, the presence of insoluble oxide forming a oxide film on the electrode surface causing blockage which occur by using neutral electrolyte can be prevented by replacing the electrolyte with alkaline electrolyte for aluminium-air batteries (Fan, Lu and Leng, 2015).

Furthermore, Ma et al have thoroughly investigated the corrosion behaviour of aluminium alloy in various solutions, including 1 M HCl, different pH levels of 0.6 M NaCl, and 4 M NaOH. The findings revealed that the alloy's corrosion response was significantly influenced by the presence of chloride ions ( $Cl^-$ ), hydroxide ions ( $OH^-$ ), and the pH of the solutions. General and pitting corrosion were observed in both acidic and neutral condition. The results demonstrate that when an alkaline solution was used, general corrosion was occurred in the alloy due to the destruction of the protective oxidation layer on the surface of alloy, whereas the use of a chloride solution led to pitting



corrosion in the alloy. Other than that, Ma et al. have concluded the value of corrosion current for different types of solution and found out that using 0.6 M HCl in pH 7 provide the lowest corrosion current at a value of  $2.33 \times 10^{-6} \text{ Acm}^{-2}$  compared to the 4M NaOH with a highest corrosion current with  $9.348 \times 10^{-3} \text{ Acm}^{-2}$ . Hence, the corrosion rate is highest in 4M NaOH, followed by 1 M HCl, then 0.6 M HCl at pH 11, with the subsequent condition at pH 4, and the lowest rate observed in 0.6 M HCl at pH 7. (Ma et al., 2013).

The experiment of Rota et al have shown that acidic electrolyte can reduce the resistance of electrolyte which indicate that higher power densities are achievable and minimize the effect of carbonation. (Rota et al., 1995) However, Liu et al. have stated that the low stability of aluminium anode in most acidic electrolytes may also causing the corrosion problems. Therefore, most of the aluminium-air battery will prefer using alkaline electrolytes than acidic electrolytes (Rota et al., 1995).

## **2.5.2 Non-Aqueous Electrolyte**

Goel et al.'s research in 2020 underscores the numerous advantages presented by non-aqueous electrolytes. These benefits encompass higher energy density, decreased anodic corrosion rates, and elevated battery voltages, collectively serving as crucial factors in mitigating the typical limitations associated with aqueous electrolytes during the development of secondary aluminium-air batteries (Goel, Dobhal and Sharma, 2020). Additionally, their findings indicate that non-aqueous electrolytes offer a viable solution to the challenge of reduced ionic conductivity arising from solid particle formation (Goel, Dobhal and Sharma, 2020). In essence, non-aqueous electrolytes can be categorized into two primary types: ionic liquid electrolytes and semi-solid or solid electrolytes.

### **2.5.2.1 Ionic liquid Electrolyte**

A number of research have been conducted to investigate the performance of ionic liquid electrolytes for aluminium battery. For instance Levy et al. have studied the tetrabutylammonium dihydrogen trifluoride ( $TBAH_2F_3$ ) ionic liquid-based electrolytes for aluminium air battery. The study's findings indicate that  $TBAH_2F_3$ -based electrolytes lead to rapid

activation of aluminium surfaces and high anodic currents, with the formation of a protective  $Al_xO_yF_z$  layer. Furthermore, the study delves into the importance of air cathode wetting for achieving high discharge potentials and identifies active fluoro-hydrogenated species during discharge. In summary, the experiment have proved that the use of  $TBAH_2F_3$ -based electrolytes resulted in high cell capacities (over 70% of the theoretical value) (Levy et al., 2020). Levy, N.R. et al. also have investigated the utilization of  $AlCl_3$  /EMImCl room temperature ionic liquid (RTIL) electrolyte on aluminium-air secondary battery. The aluminium-air battery shows a remarkable reduction in self-discharge rates, establishing itself as a dependable and self-sustaining energy source. It can withstand high current densities, reaching up to  $0.6 \text{ mAcm}^{-2}$ , while maintaining an average voltage range of 0.6 V to 0.8 V. Importantly, it exhibits an impressive capacity of  $71 \text{ mAhcm}^{-2}$  at  $0.1 \text{ mAcm}^{-2}$ , surpassing the performance of conventional lithium-ion batteries by five to ten times (Levy et al., 2020).

In the experiment conducted by Gelman et al., they utilized a 1-ethyl-3-methylimidazolium oligo-fluorohydrogenate ( $EMIm(HF)_{2.3}F$ ) electrolyte in an aluminium-air battery to assess both its anodic and cathodic performance. The findings revealed that the battery could effectively harness over 70% of its theoretical aluminium capacity, achieved by elevating the current densities to levels exceeding  $1.5 \text{ mAcm}^{-2}$ . Moreover, they have discovered that the aluminium anode undergoes a process that results in the creation of an Al-O-F layer on its surface when using the  $EMIm(HF)_{2.3}F$  electrolyte. This Al-O-F layer formation, in turn, facilitates the activation of the anode and contributes to the achievement of low corrosion rates for the aluminium anode. Additionally, they also compared between aluminium-air batteries employing aqueous and non-aqueous electrolytes. The results demonstrated that the battery utilizing the non-aqueous ionic liquid electrolyte outperformed its aqueous counterpart in terms of practical gravimetric energy density, practical volumetric energy density, and corrosion current. Particularly noteworthy was the minimal corrosion observed on the Al anode in the ionic liquid, making this proposed

system highly appealing due to its enhanced electrode utilization (Gelman, Shvartsev and Ein-Eli, 2014).

### 2.5.2.2 Semi-solid and solid electrolytes

The adoption of semi-solid and solid electrolytes in various battery applications is gaining traction as a promising alternative to traditional liquid electrolytes. This shift is primarily driven by the demonstrated potential to enhance both stability and safety in all-solid-state batteries (ASSBs). According to Zheng et al.'s research analysis, the principal issue with liquid electrolytes pertains to their inherently low thermal stability, which poses significant safety concerns (Zheng et al., 2018). Correspondingly, Liang et al. highlighted similar concerns within lithium-ion batteries, where the majority of electrolytes exhibit low boiling points (below 300 °C) and flash points (below 150 °C). These characteristics contribute to the thermal instability, volatility, and flammability of organic liquid electrolytes, which are key factors underlying the safety challenges associated with LIBs (Liang et al., 2019). Therefore, Zheng et al. consolidated the benefits of transitioning to ASSBs over the use of liquid electrolytes. First and foremost, this transition results in an augmented energy density, thanks to the substantial reduction in the battery's dead weight without liquid electrolytes. Additionally, the adoption of inorganic solid electrolytes enhances electrochemical stability and enables compatibility with various cathode materials. Lastly, ASSBs exhibit significantly improved mechanical properties (Zheng et al., 2018).

In one of the experiments conducted by Mori, the focus was on investigating a semi-solid-state aluminium-air battery employing a solid electrolyte consisting of mixtures containing  $AlCl_3 \cdot 6H_2O$ . During this experimental phase, various hydrophobic additives were introduced into the solid electrolyte, including tetrabutylphosphonium hexafluorophosphate, vaseline, dimethicone/vinyl dimethicone crosspolymer, triethanolamine stearate, and vaseline, along with butyl methyl imidazolium hexafluorophosphate, to prevent liquefaction under ambient conditions. The outcomes revealed that when vaseline and butyl methyl imidazolium hexafluorophosphate were included as additives in the solid electrolyte, the Al-air battery demonstrated a

sustained high current output over an extended duration. This underscores the practical viability of this semi-solid-state Al-air battery as a promising candidate for real-world applications (Mori, 2018).

In addition, Z. Zhang et al. have presented an all-solid-state aluminium-air battery featuring an alkaline gel constructed with polyacrylic acid (PAA). This gel electrolyte achieves a noteworthy ionic conductivity of  $460 \text{ mS cm}^{-1}$ , displaying striking similarities to the performance of conventional aqueous electrolytes. During continuous discharge at a constant current, the aluminium-air battery demonstrates outstanding capacity and energy density metrics, reaching  $1166 \text{ mAh g}^{-1}$  and  $1230 \text{ mWh g}^{-1}$ , respectively, accompanied by an impressive power density of  $91.13 \text{ mW cm}^{-2}$ . Furthermore, Z. Zhang et al.'s research has revealed that mitigating anodic corrosion can be achieved by physically isolating the Al anode from the gel electrolyte during periods of inactivity, effectively preserving the battery's available capacity. (Zhang et al., 2014b).

## 2.6 Summary

Aluminum-air batteries have garnered attention as efficient and sustainable energy storage systems. The choice of anode material, either pure aluminium or aluminium alloys, influences battery performance, with pure aluminium offering high energy density and alloys providing corrosion resistance. Air cathodes, essential for oxygen reduction, require careful design and catalyst selection to boost efficiency. Eco-friendly cellulose-based separators enhance safety by facilitating ion transport and preventing short circuits. The choice between aqueous and non-aqueous electrolytes is crucial. Aqueous electrolytes offer high ionic conductivity but face corrosion and water loss issues, whereas non-aqueous electrolytes mitigate these problems, enhancing performance. In essence, aluminium-air battery development is complex, with anodes, cathodes, separators, and electrolytes all vital for optimizing performance, energy density, and sustainability across applications.

## CHAPTER 3

### METHODOLOGY AND WORK PLAN

#### 3.1 Introduction

This section provides an overview of the materials and equipment needed for our study. The fabrication material and process of the specific cellulose-based separator for the aluminium coin cell battery are emphasized in this chapter. Furthermore, the complete fabrication process of the aluminium coin cell battery and the assembly procedure are explained in detail. Lastly, the flowchart of the work plan for the study is shown in Figure 3.1, and our work plan is presented from Figures 3.8 to 3.11 using a Gantt chart.

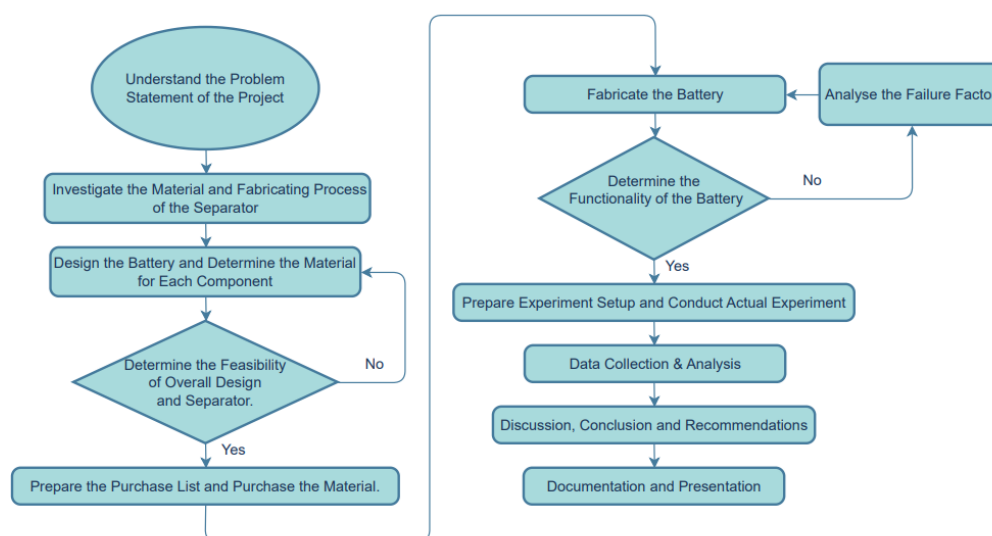


Figure 3.1: Work Plan Flowchart

#### 3.2 Material Preparation

The materials used in the fabrication of an aluminium coin cell battery were carefully prepared to ensure optimal performance. The material of the anode is aluminium 6061 plate, while the cathode featured a combination of materials, including nickel-mesh, activated carbon (AC), carbon black (CB), manganese dioxide ( $MnO_2$ ), Polytetrafluoroethylene (PTFE) and Propanol. The electrolyte utilized was KOH, facilitating the ion exchange necessary for the battery's operation. The separator of battery was created using a mixture of

Carboxymethyl cellulose (CMC), Polyvinyl Alcohol (PVA), and Nanofibrils Cellulose (CNF) from conifer plant.

### 3.3 Overall Design of Battery

Figure 3.2 shows the overall design for the aluminium coin cell battery. There are several parts included in the overall design including positive case, cathode, separator, anode, spacer, spring and negative case.



Figure 3.2: Overall design of aluminium-air battery.

Figure 3.3 illustrates the comprehensive assembly procedure of the coin cell battery, encompassing all housing components and battery constituents.

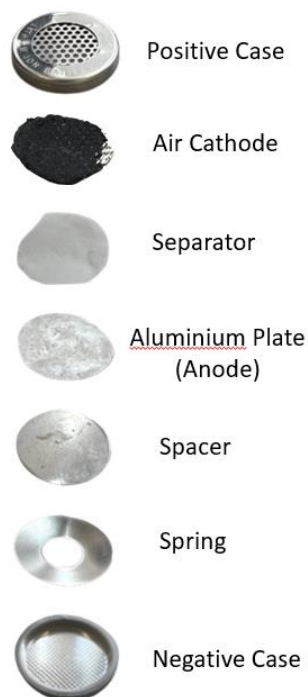


Figure 3.3: Overall Assembly Process of the coin cell battery.

### 3.4 Preparation of Electrolyte

First, prepare 2.81 g KOH pellets with 50 ml of distilled water to produce 1 M KOH solution. After that, mix them and keep stirring until the pellets are fully dissolved in the distilled water.

### 3.5 Preparation of Aluminium Anode

Prepare the aluminium 6061 plate with 0.2 mm of thickness and cut into a circular shape with a diameter of 19 mm to act as an aluminium anode.

### 3.6 Preparation of Air Cathode

First of all, prepare the catalyst mixture by mixing activated carbon (AC), carbon black (CB), and manganese dioxide ( $MnO_2$ ) in a ratio of 8:1:1 and stir the mixture thoroughly. Next, mixing PTFE solution and Propanol solution into the catalyst mixture, stirring continuously until the catalyst mixture fully dissolves into the solution. This will result in a paste-like solution that can be evenly spread onto the surface of the nickel mesh.

### 3.7 Preparation of Separator

In this study, two different types of separators were employed. Firstly, a homogeneous solution was created by dissolving nanofibril cellulose (CNF) and CMC in a weight ratio of 85:15, 75:25 and 65:35 in 5 ml of distilled water. The mixture was mixed with a rotor-stator mixer at a speed of 600 rpm for one hour until it reached a homogeneous state. The resulting solution was then poured into multiple Petri dishes and underwent a freeze-thawing process in chest freezer at  $-10^{\circ}\text{C}$  for 24 hours. To confirm the absence of water or gel formation, the film underwent further drying in a desiccator. This preparation process was proposed by Zainuddin et al. (Zainuddin et al., 2018).

The second type of separator used in this study consisted of nanofibril cellulose (CNF) combined with PVA as the binder in a ratio of 85:15 wt% , 75:25wt% and 65:35 wt%, making a total mass of 0.3 g of cellulose. The mixture was mixed with a rotor-stator mixer at a speed of 600 rpm for one hour until it reached a homogeneous state. Then, the mixture was poured into a petri dish

and underwent a freeze-thawing process in chest freezer at  $-10^{\circ}\text{C}$  for 24 hours. Subsequently, the separator was further dried at room temperature for one day until it was completely dry. This preparation process was proposed by Selan et al. (Selan et al., 2023)

After that, the study proceeded to scale up the production of both types of separators while maintaining the same weight ratios. For the first type of separator, the quantities of nanofibril cellulose (CNF) and carboxymethyl cellulose (CMC) were doubled while preserving the weight ratios of 85:15, 75:25, and 65:35 in 10 ml of distilled water. Similarly, for the second type of separator, the amounts of CNF and polyvinyl alcohol (PVA) were doubled while maintaining the weight ratios of 85:15, 75:25, and 65:35 to make a total mass of 0.6 g of cellulose.

### **3.8 Testing**

To begin, the battery's discharge performance is assessed using VersaSTAT4 Potentiostat Galvanostat. The discharge test involves discharging the battery at a current of 20mA until the battery's electrolyte is depleted. Subsequently, an I-V curve is generated and the total discharge time is recorded to calculate the discharge capacity.

Additionally, a linear sweep voltammetry (LSV) test is conducted on the battery using potentiostat to obtain a polarization curve. The LSV test involves setting the voltage scan rate to a specific value of  $5\text{ mVs}^{-1}$  and setting the initial potential at open circuit voltage of the assembled cell. During the test, the current response is collected as the potential is linearly increased, allowing for an analysis of the battery's performance.



## CHAPTER 4

### RESULTS AND DISCUSSION

#### 4.1 Introduction

This section provides a summary of the experimental results obtained by using numerous types of separators, each created with a different binder. Subsequently, the most effective separator was chosen for the production of the best coin cell battery, and its performance was evaluated using discharging and linear sweep voltammetry tests. The results of these tests are discussed in the final portion of this chapter.

#### 4.2 Performance of the separators

We designed a basic aluminium-air battery test model to compare the performance of two types of separators with different cellulose and binder weight ratios. The model was made of acrylic board, with an air cathode as the cathode and a 5mm thick aluminium plate 6061 as the anode, to assess the separator's performance. One of the binders utilized was polyvinyl alcohol (PVA), while the other was carboxymethyl cellulose (CMC). The weight ratios of cellulose to binder were set to 85:15, 75:25, and 65:35 for each separator type.

##### 4.2.1 Cellulose separators with PVA binder

Three separators were made with varied weight ratios of nanofibril cellulose (CNF) and polyvinyl alcohol (PVA) binder, totalling 0.3 grams, and combined with 5 millilitres of distilled water. The separators have been designated based on the weight combinations of CNF and PVA shown in Tables 4.1 and 4.2 below. The three separators were then combined into an aluminium-air battery test model for discharge testing and linear sweep voltammetry measurement to evaluate their performance. Figures 4.1 and 4.2 show the discharge performance curve and linear sweep voltammetry curve for each separator version, allowing for a study of the effect of varied weight ratios on discharge behaviour.

Table 4.1: Separator Composition and Corresponding Masses

Separators	CNF(g)	PVA(g)	Distilled Water(ml)
CNF85:PVA15	0.255	0.045	5
CNF75:PVA25	0.225	0.075	5
CNF65:PVA35	0.195	0.105	5

Table 4.2: Comparison Table of Separators Utilizing PVA Binder

Separators	Discharge time(s)	Plateau Voltage(V)	Peak Power(mW)
CNF85:PVA15	126	-	22
CNF75:PVA25	554	1.25	21
CNF65:PVA35	679	0.95	36

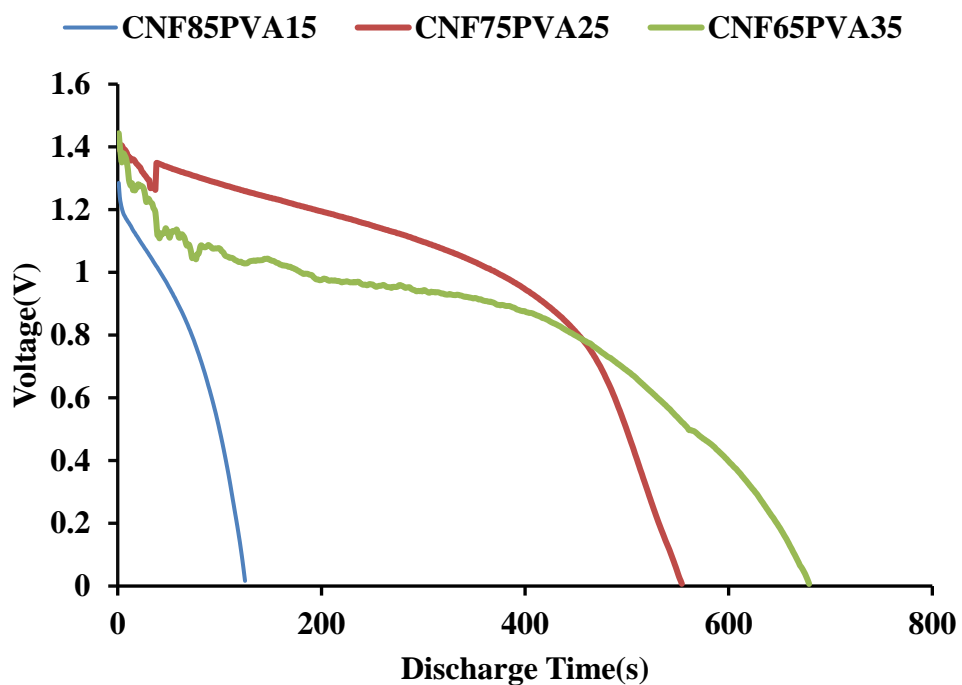


Figure 4.1: Discharge Curve with Varied Separator Weight Ratios with PVA binder

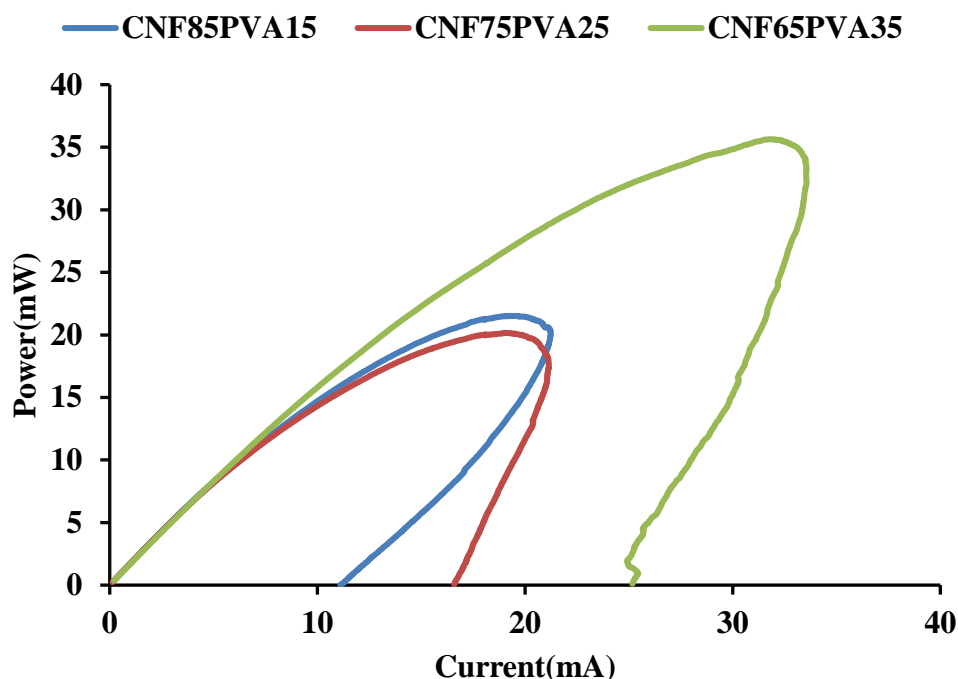


Figure 4.2: LSV Curve with Varied Separator Weight Ratios

First and foremost, the three curves in Figure 4.1 above depict the discharge performance behaviour of three distinct cellulose separators with PVA binder at discharge current of 20mA. According to the graph, the discharge behaviour of both CNF75:PVA25 and CNF65:PVA35 separators is comparable but differs from the CNF85:PVA15 separator. For the battery with the CNF85:PVA15 separator, there is a fast and continuous decline in voltage with no periods of stabilization. This showed that the absence of voltage plateaus occurred throughout the discharge operation. Unlike the CNF85:PVA15 separator, the other two separators, CNF75:PVA25 and CNF65:PVA35, exhibit voltage plateaus throughout the discharge process, albeit at varying values.

In addition, the CNF85:PVA15 separator takes much additional time than the other two separators to completely deplete the battery to 0V. The experiment results, which may be found in Table 4.2, suggest that a larger PVA binder ratio corresponds to a longer discharge time for the battery at a given discharge current value. The battery with separators and additions of 15%, 25%, and 35% PVA produced discharge capacities of 250 mAh/g, 716 mAh/g, and 920 mAh/g, respectively, according to calculations. This suggests that

increasing the weight percentage of binder from 15% to 35% can improve battery discharge performance and increase battery life.

The absence of voltage plateaus and quick depletion in the battery can be attributed to cellulose's strong retention within the separator material. Excessive retention occurs when the cellulose material expands significantly, preventing the battery from functioning properly. This phenomena is caused by cellulose's natural hydrophilicity, as seen by its hydroxyl (-OH) and carboxyl (-COOH) groups, which readily form hydrogen bonds with water molecules. As highlighted by Olejnik et al. and Etale et al., this swelling happens when water molecules enter the disordered portions of the semi-crystalline cellulose structure, forming hydrogen bonds with the hydroxyl groups on the glucose chains.(Olejnik et al., 2017; Etale et al., 2023) As a result, the cellulose's volume and thickness grow. The thickness of the separator increases the internal resistance by introducing additional barriers to ion transport, limiting ion movement between electrodes, impeding the battery's ability to sustain high discharge rates and causing rapid discharge, thereby limiting overall performance. Moreover, Maksimov et al. conducted an experiment to show that swelling raises the cell's internal resistance, affecting battery performance. (Maksimov et al., 2023)

One of the simple ways to reduce the effect of the swelling is by increasing the concentration of binder. The reason for having a better performance for CNF65:PVA35 separator is due to the impact of the high concentration of PVA binder. The concentration of binders in cellulose film formulations plays a critical role in determining the performance of batteries. Increase the concentration of binder can improve the mechanical properties of cellulose separator by enhancing the tensile strength , durability and so on. This is because binders can strengthen the adhesion of cellulose to ensure better bonding between each other.

Apart from that, the curves in Figure 4.2 above show the battery's performance during the LSV test. Based on the graph, the results show that the

peak power for CNF65:PVA35 is significantly higher than others, indicating that the battery with CNF65:PVA35 separator can generate more power output for a given current, which can be useful in applications requiring high power output or fast energy transfer. However, after reaching peak power, the current for all separators using PVA binder in the LSV test decreased somewhat. This is due to the limitation of the mass transport which means that at the peak current densities the ions transport in the battery is limited significantly leading to a result in reduced diffusion rates of ions or reactants to the electrode surface.

#### 4.2.2 Cellulose separators with CMC binder

Three separators were made with varied weight ratios of nanofibril cellulose (CNF) and carboxymethyl cellulose (CMC) binder, comprising 0.3 grams and combined with 5 milliliters of distilled water. The separators were labeled based on the weight combinations of CNF and CMC shown in Tables 4.3 and 4.4 below. The three separators were then combined into an aluminum-air battery test model for discharge testing and linear sweep voltammetry measurement to evaluate their performance. Figures 4.3 and 4.4 show the discharge performance curve and linear sweep voltammetry curve for each separator version, allowing for a study of the effect of varied weight ratios on discharge behaviour.

Table 4.3: Separator Composition and Corresponding Masses(CMC binder)

Separators	CNF(g)	CMC(g)	Distilled Water(ml)
CNF85:CMC15	0.255	0.045	5
CNF75:CMC25	0.225	0.075	5
CNF65:CMC35	0.195	0.105	5

Table 4.4: Comparison Table of Separators Utilizing CMC Binder

Separators	Discharge time(s)	Plateau Voltage(V)	Peak Power(mW)
CNF85:CMC15	451	1.05	35
CNF75:CMC25	656	0.75	27
CNF65:CMC35	363	0.65	24

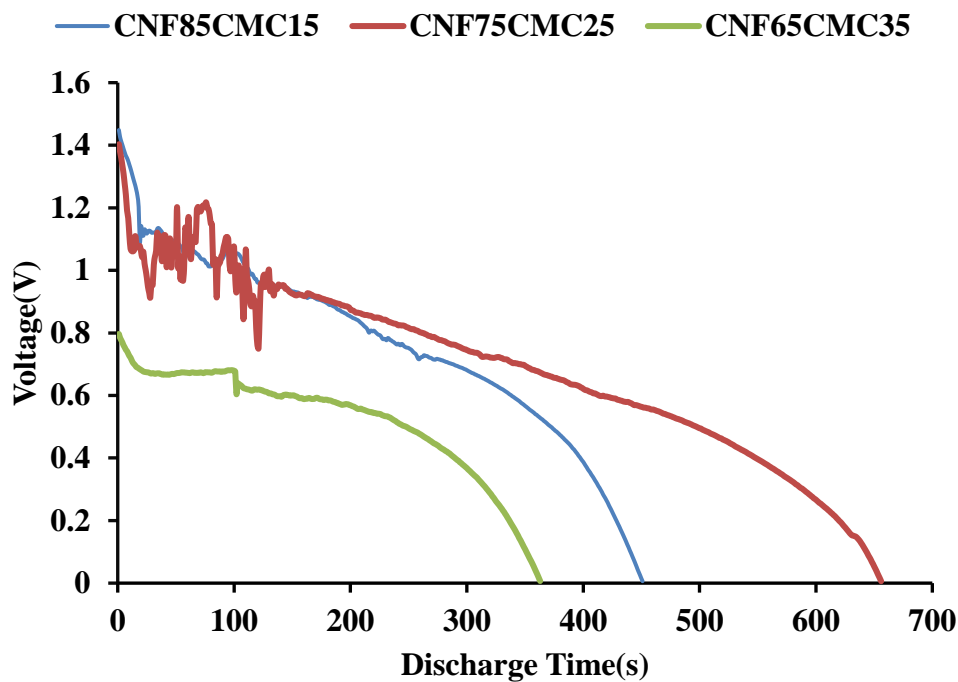


Figure 4.3: Discharge Curve with Varied Separator Weight Ratios with CMC binder

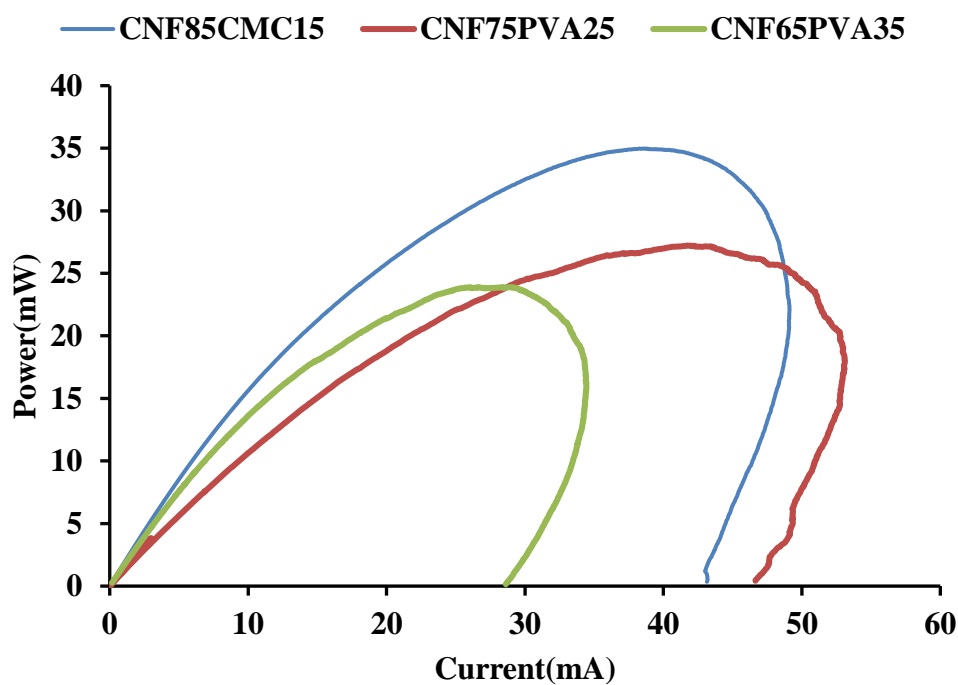


Figure 4.4: LSV Curve with Varied Separator Weight Ratios with CMC binder

The current investigation looked at the influence of various weight ratios of nanofibril cellulose (CNF) and carboxymethyl cellulose (CMC) binder separators. Figure 4.3 above depicts the discharge behaviour for each separator. According to the data, CNF75:CMC25 separators with a 25% CMC binder weight percentage beat other separators, with a discharge time of 656 seconds compared to CNF85:CMC15 and CNF65:CMC35, which had discharge times of 451 and 363 seconds, respectively. Calculations revealed that the batteries with separators containing 15%, 25%, and 35% CMC had discharge capacities of 840 mAh/g, 878 mAh/g, and 330 mAh/g, respectively.

According to the discharge and LSV curves, the battery with the CNF65:CMC35 separator has the lowest performance compared to the others. This is owing to the poor ionic conductivity, which means that ions travel less efficiently through the cellulose separator than through other materials. This can be compromised if the concentration of the CMC binder is too high and the concentration of cellulose is too low, causing the separator to become too dense and compact. This lowers the number of accessible ion transport channels, making electrolyte penetration and diffusion more difficult. As a result, the battery's performance may be affected, resulting in shorter discharge times and worse overall efficiency.

### **4.3 Cellulose Separators with Doubled Total Mass Utilizing CMC or PVA Binders**

In the current study, the effect of doubling the total mass of cellulose separators to 0.6g for both polyvinyl alcohol (PVA) and carboxymethyl cellulose (CMC) binders was studied while keeping the weight ratio constant. The weight ratios of cellulose nanofibrils (CNF) to binder were kept constant at 85:15, 75:25, and 65:35 for both PVA and CMC binders. The separators' double mass was accomplished by increasing the number of cellulose nanofibrils and binder components while leaving the remaining experimental settings unchanged. The separators were marked based on the weight combinations of CNF and PVA or CMC, as shown in Tables 4.5 and 4.6 below.

Table 4.5: Separator Composition and Corresponding Masses (PVA binder)

Separators	CNF(g)	PVA(g)	Distilled Water(ml)
CNF85:PVA15	0.51	0.09	10
CNF75:PVA25	0.45	0.15	10
CNF65:PVA35	0.39	0.21	10

Table 4.6: Separator Composition and Corresponding Masses(CMC binder)

Separators	CNF(g)	CMC(g)	Distilled Water(ml)
CNF85:CMC15	0.51	0.09	10
CNF75:CMC25	0.45	0.15	10
CNF65:CMC35	0.39	0.21	10

Table 4.7: Comparison Table of Doubled Separator Masses Separators

Utilizing different binders.

Separators	Discharge time(s)	Plateau Voltage(V)	Peak Power(mW)
CNF85:PVA15	848	0.85	26
CNF75:PVA25	386	1.15	15
CNF65:PVA35	511	1.15	30
CNF85:CMC15	442	0.95	31
CNF75:CMC25	1121	1.15	48
CNF65:CMC35	733	0.95	23



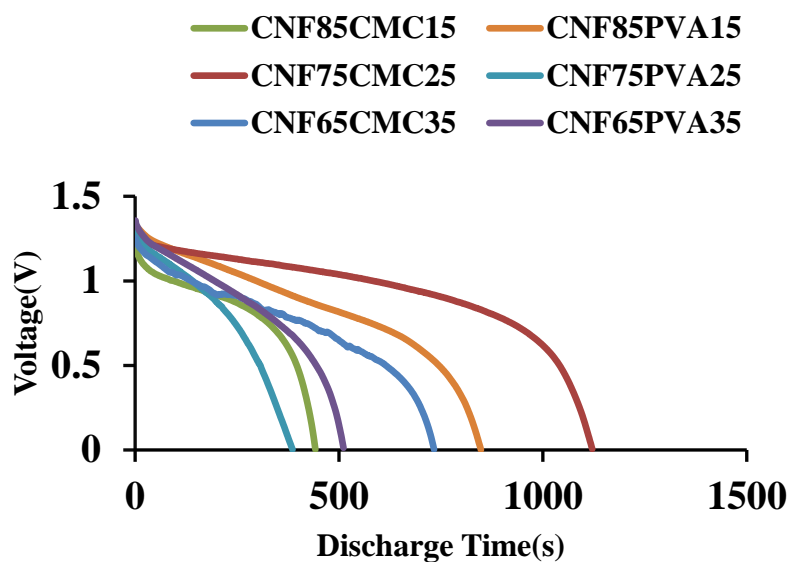


Figure 4.5: Discharge Curve with Doubled Separator Masses and Varied Weight Ratios of both PVA and CMC Binders

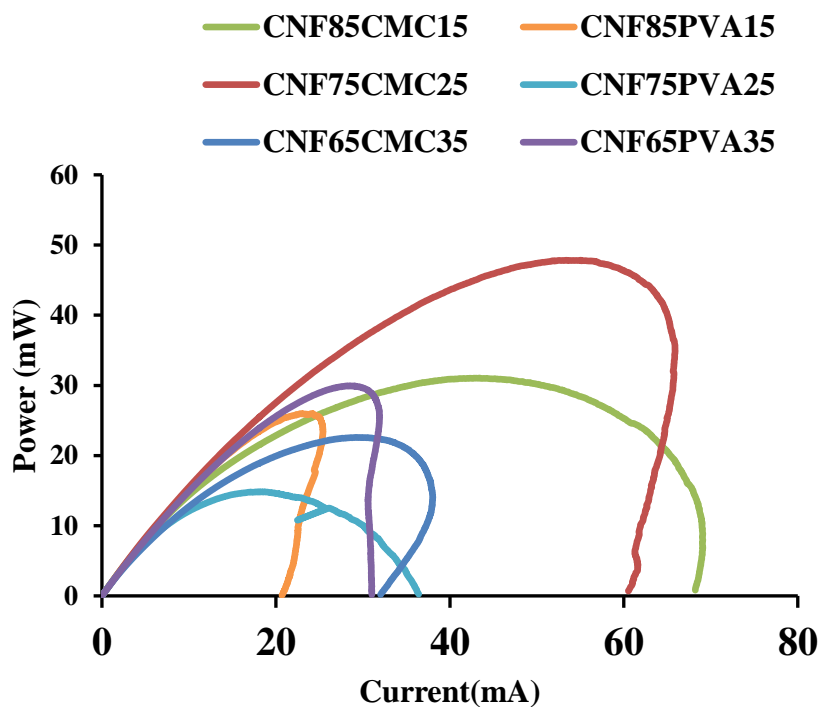


Figure 4.6: LSV Curve with Doubled Separator Masses and Varied Weight Ratios of both PVA and CMC Binders

According to the findings, all separators in this investigation exhibit identical discharge behaviour, albeit at various discharge time. Despite variances in composition and binder type, the discharge curves for all separators show identical tendencies, with an initial voltage plateau followed by a slow drop until reaching the endpoint voltage. Separators made with CMC binders, which are 75% CNF and 25% CMC by weight, stand out for their higher performance, with a discharge duration of 1121 seconds under a 20mA discharge current, indicating that the battery would operate for a longer period of time before reaching its endpoint voltage. Furthermore, it has the highest plateau voltage reported at 1.15V during discharge. Furthermore, CNF75CMC25 with doubled mass had the maximum power at 47.8mW during the LSV test.

By comparing these separators to previous separators, the results revealed that increasing the overall mass of cellulose separators while retaining the same weight ratio of CNF to binder had a significant impact on the separators' performance. One of the instances is illustrated in Figure 4.7, which depicts the discharge behaviour of a CNF75CMC25 separator with different total masses, one of which is 0.3g and the other is 0.6g. By analyzing the discharge curve, the CNF75CMC25 separator with 0.6g outperformed the separator with 0.3 in terms of discharge time and plateau voltage. Furthermore, the LSV curve plotted in Figure 4.8 shows a similar tendency in that the peak power of the separator with 0.6g but the same weight ratio is much higher than another, supporting the assertion.

All separators with the same weight ratio and binder but doubled mass will considerably enhance battery performance, resulting in longer discharge times and higher peak power. The additional mass resulted in thicker separators, which may improve mechanical stability and electrolyte retention within the battery. Thicker separators may also provide better physical protection for the electrodes, lowering the possibility of a short circuit during battery operation. As a result, the swelling impact can be reduced, allowing the separator to be more robust when immersed in electrolytes.

However, the separator made of nanofibril cellulose (CNF) and carboxymethyl cellulose (CMC) in a 75:25 ratio with a mass of 0.6g demonstrated a discharge time of 1121 seconds under a 20mA discharge current in this study. This performance is significantly poorer when compared to previous studies. For example, Selan et al. described a separator made of water hyacinth cellulose nanofibrils and polyethylene glycol 400 (PEG 400) binder in an 85:15 wt% ratio, attaining a total discharge time of roughly 18471 seconds under a 10mA discharge current. (Selan et al., 2023) Furthermore, Tan et al. found that a polypropylene separator produced a discharge duration of approximately 3780 seconds at a discharge current of 20mA. (Tan et al., 2021)

One significant factor contributing to the lower performance of the CNF separator with CMC binder in this research is the source of the nanofibril cellulose. The cellulose was produced from coniferous sources. Conifer-derived cellulose often has distinct structural and chemical properties than cellulose generated from other plant sources, such as water hyacinth. These variances can influence the separator's mechanical strength, porosity, and overall electrochemical performance. Conifer-derived cellulose may have fewer desirable qualities for battery applications than cellulose produced from sources such as water hyacinth, which Selan et al. used in their high-performance separator.

Another reason for the observed lower performance is the material composition and ratio used in the CNF separator with CMC binder. The separator's characteristics may not be optimized for battery applications when nanofibril cellulose and carboxymethyl cellulose are combined in a 75:25 ratio. When compared to other composites, carboxymethyl cellulose may decrease the overall ionic conductivity and mechanical integrity of the separator, despite the fact that it is frequently included to increase flexibility and processability. On the other hand, it's possible that Selan et al.'s use of polyethylene glycol 400 as a binder enhanced ionic conductivity and stability, leading to noticeably longer discharge times. PEG 400 is well-known for its strong plasticizing action and

excellent ionic conductivity, both of which can improve the separator's performance.

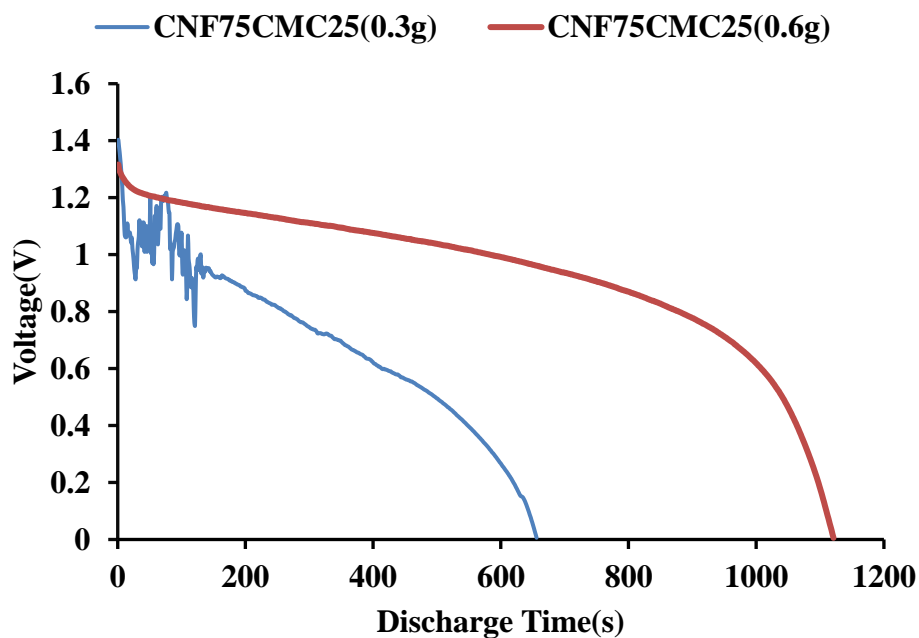


Figure 4.7: Discharge Curves for CNF75CMC25 Separator with Varied Total Mass

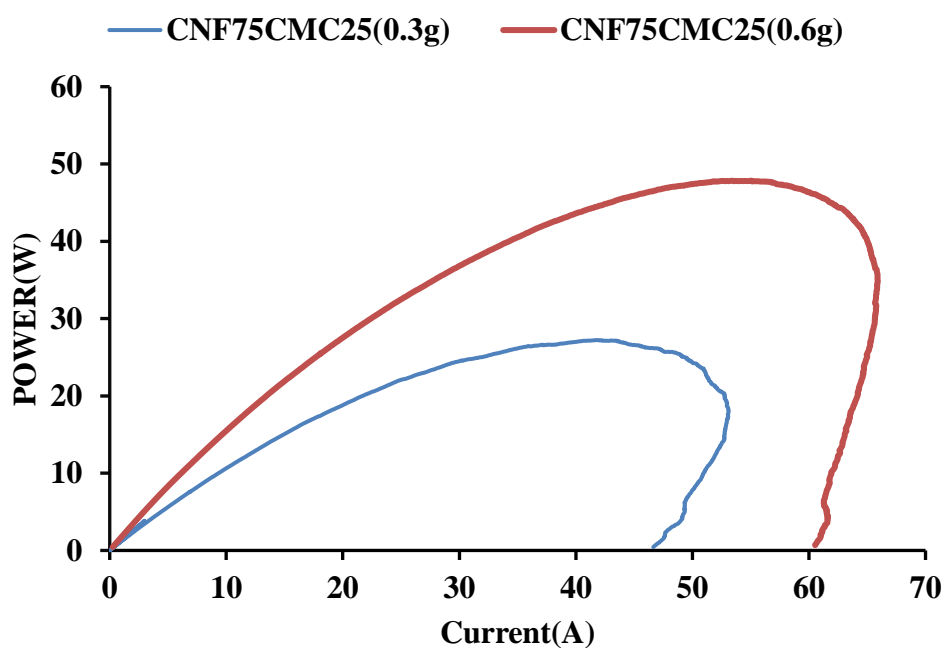


Figure 4.8: LSV Curves for CNF75CMC25 Separator with Varied Total Mass

#### 4.4 Coin Cell Battery Characterization

This section focused on the aluminium air coin cell battery. The battery is built with an aluminum plate as the anode, an air cathode, CNF75CMC25 separators with doubled mass, and KOH as the electrolyte. The battery was attached to an electrochemical workstation to analyze its charge and discharge performance. The battery was discharged at 10 mA until the discharge potential was zero. The discharge curve was represented by the graph in Figure 4.9 below. The coin cell battery was tested using the LSV test with a voltage scan rate of  $5 \text{ mVs}^{-1}$ . Figure 4.10 above shows the power against current curve.

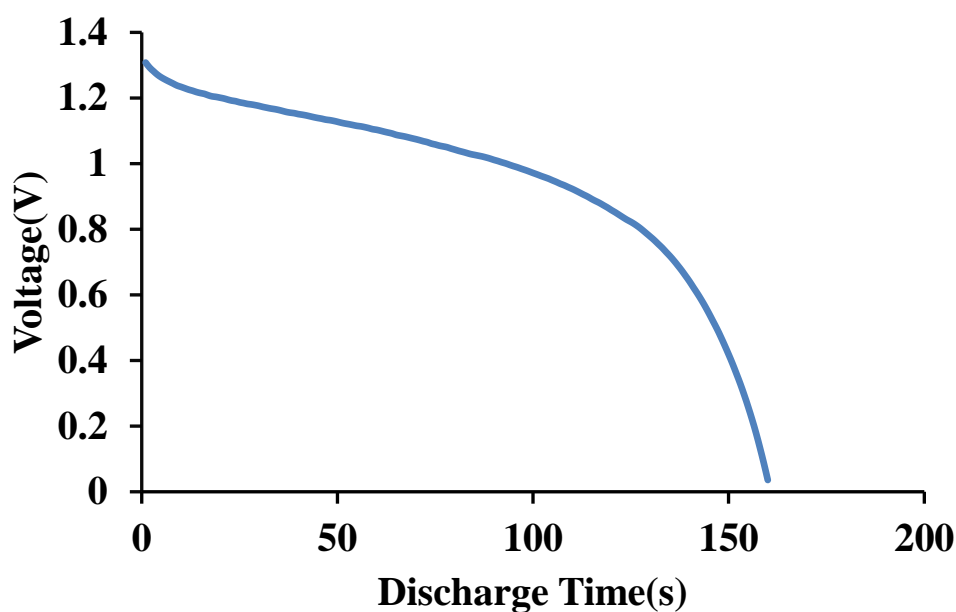


Figure 4.9: Discharge Curve of Coin Cell Battery Utilizing Optimal Separator Composition

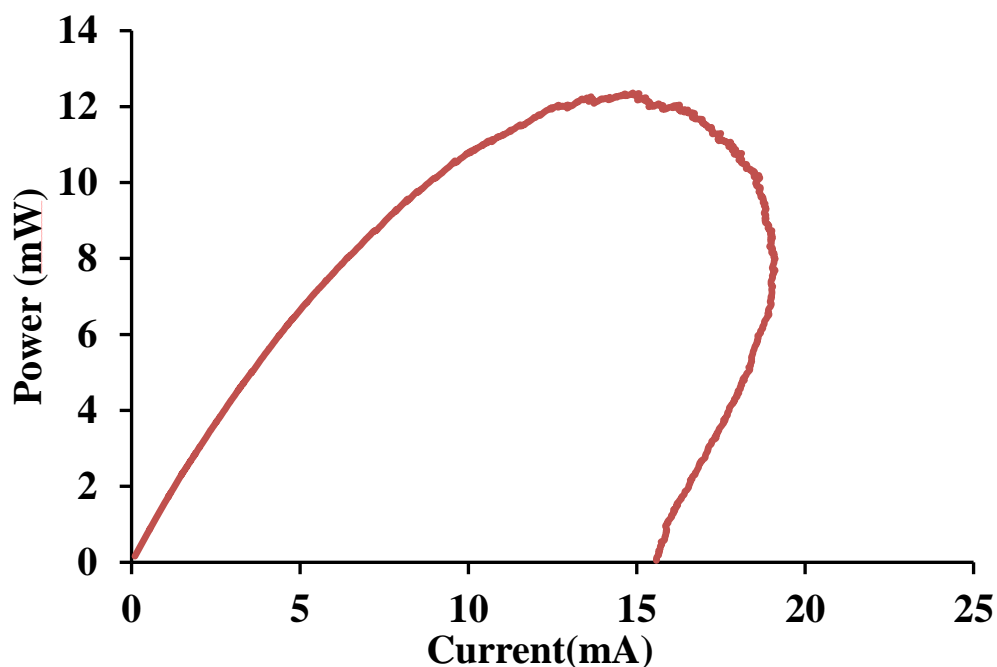


Figure 4.10: LSV Curve of Coin Cell Battery Utilizing Optimal Separator Composition

According to the discharge curve given in Figure 4.9 above, the curve begins with the discharging operation and then shows a quick fall in potential after 130 seconds, indicating a major shift in the battery's discharge behavior at that time point. This quick reduction in potential indicates a sudden drop in the battery's voltage output, resulting in a short discharge time of only 160 seconds for 10mA. Furthermore, the LSV curve displayed in Figure 4.10 above revealed that the peak power of the coin cell battery is 12.4mW, which is regarded poor performance for a coin cell battery.

The low performance reported in our investigation is due to the considerable pressure exerted on the separator within the coin cell arrangement. This increased pressure causes mechanical stress on the separator material, resulting in structural collapse and short-circuiting of the battery. As a result, the discharge duration is substantially shorter, and the peak power is lower than in typical conditions. This condition is also supported by Aiello et al.'s experiment, which showed that the best performance of LIB can be achieved at lower pressures. An external mechanical compression and the resulting increase

in the LIB inner resistance, due to separator pores occlusion, may result in a less significant increase in the inner impedance. (Aiello et al., 2024) In addition, Mussa et al. studied the effects of external pressure on fuel cell performance and discovered that capacity decreases at high pressure, implying that excessively high pressure has a detrimental impact on the performance of the pouch cell.(Mussa et al., 2018) As a result, additional improvements are required to boost the strength of the separator.

## CHAPTER 5

### CONCLUSION AND RECOMMENDATION

#### 5.1 Conclusion

The study evaluated cellulose separators with different binders and weight ratios in aluminum-air battery systems through discharge testing and linear sweep voltammetry (LSV). Results showed significant performance variations based on binder type, weight ratio, and total mass. CMC binders generally led to shorter discharge times and lower plateau voltages compared to PVA binders due to differing properties affecting ion transport and separator stability. Doubling total mass while maintaining the same weight ratio resulted in considerable performance improvements, particularly in CMC binders, with longer discharge durations and higher peak powers. The separator with the best performance in this study is the separator with CMC binders, composed of 75% CNF and 25% CMC by weight, with a total mass of 0.6g. During the discharge test, this separator exhibited a discharge time of 1121 seconds at a 20mA discharge current, along with the highest plateau voltage at 1.15V. In the LSV test, it reached a peak power of 47.8mW. Finally, the CNF75CMC25 separator with 0.6g was utilized as the separator for an aluminum coin cell battery, achieving a discharge time of 160 seconds and a plateau voltage of 1.15V. The peak power of the coin cell battery was measured at 12.4mW.

#### 5.2 Recommendation

Through this research, there are many ways to improve the performance of cellulose-based separators and coin cell batteries. To start with, raising the binder concentration in cellulose separators has the potential to greatly improve mechanical strength and stability. This increased concentration would promote greater adhesion between cellulose fibers, improving overall separator performance.

Aside from that, crosslinking agents like urea, citrus acid, or tannic acid should be used in the cellulose-based separator. This is because adding crosslinking agents can improve the structural integrity of cellulose separators.



These chemicals encourage crosslinking between cellulose molecules, producing in a stronger separator structure that is resistant to mechanical stress and swelling.

Furthermore, alternative binder materials that outperform classic binders like PVA and CMC in terms of mechanical qualities and chemical stability should be studied. This could entail looking into innovative polymers or natural additions that improve separator performance without affecting other battery properties.

Last but not least, it is vital to build reinforced separator structures that can survive the high pressures encountered in coin cell batteries. Designing separators with strengthened layers or structural upgrades can successfully prevent separator breakage and short circuits. These adjustments can greatly increase coin cell battery reliability and performance, ensuring optimal operation even in tough settings.

## References

- Aiello, L., Ruchti, P., Vitzthum, S. and Coren, F., 2024. Influence of Pressure, Temperature and Discharge Rate on the Electrical Performances of a Commercial Pouch Li-Ion Battery. *Batteries*, 10(3), p.72. <https://doi.org/10.3390/batteries10030072>.
- Chen, S., Zhang, M., Zou, P., Sun, B. and Tao, S., 2022. *Historical development and novel concepts on electrolytes for aqueous rechargeable batteries. Energy and Environmental Science*. <https://doi.org/10.1039/d2ee00004k>.
- Cheng, R., Wang, F., Jiang, M., Li, K., Zhao, T., Meng, P., Yang, J. and Fu, C., 2021. Plasma-Assisted Synthesis of Defect-Rich O and N Codoped Carbon Nanofibers Loaded with Manganese Oxides as an Efficient Oxygen Reduction Electrocatalyst for Aluminum-Air Batteries. *ACS Applied Materials and Interfaces*, 13(31), pp.37123–37132. <https://doi.org/10.1021/acsami.1c09067>.
- Cho, Y.J., Park, I.J., Lee, H.J. and Kim, J.G., 2015. Aluminum anode for aluminum-air battery - Part I: Influence of aluminum purity. *Journal of Power Sources*, 277, pp.370–378. <https://doi.org/10.1016/j.jpowsour.2014.12.026>.
- Ding, F., Zong, J., Wang, S., Zhong, H., Zhang, Q. and Zhao, Q., 2016. *3 Aluminum-Air Batteries Fundamentals and Applications*.
- Etale, A., Onyianta, A.J., Turner, S.R. and Eichhorn, S.J., 2023. *Cellulose: A Review of Water Interactions, Applications in Composites, and Water Treatment. Chemical Reviews*, <https://doi.org/10.1021/acs.chemrev.2c00477>.
- Fan, L., Lu, H. and Leng, J., 2015. Performance of fine structured aluminum anodes in neutral and alkaline electrolytes for Al-air batteries. *Electrochimica Acta*, 165, pp.22–28. <https://doi.org/10.1016/j.electacta.2015.03.002>.
- Farsak, M. and Kardaş, G., 2018. Electrolytic Materials. In: *Comprehensive Energy Systems*. Elsevier Inc. pp.329–367. <https://doi.org/10.1016/B978-0-12-809597-3.00225-X>.

Gelman, D., Shvartsev, B. and Ein-Eli, Y., 2014. Aluminum-air battery based on an ionic liquid electrolyte. *Journal of Materials Chemistry A*, 2(47), pp.20237–20242. <https://doi.org/10.1039/c4ta04721d>.

Goel, P., Dobhal, D. and Sharma, R.C., 2020. Aluminum–air batteries: A viability review. *Journal of Energy Storage*, <https://doi.org/10.1016/j.est.2020.101287>.

Huang, X., 2011. Separator technologies for lithium-ion batteries. *Journal of Solid State Electrochemistry*, <https://doi.org/10.1007/s10008-010-1264-9>.

Jana, K.K., Lue, S.J., Huang, A., Soesanto, J.F. and Tung, K.L., 2018. Separator Membranes for High Energy-Density Batteries. *ChemBioEng Reviews*, <https://doi.org/10.1002/cben.201800014>.

Kuo, Y.L., Wu, C.C., Chang, W.S., Yang, C.R. and Chou, H.L., 2015. Study of Poly (3,4-ethylenedioxythiophene)/MnO<sub>2</sub> as Composite Cathode Materials for Aluminum-Air Battery. *Electrochimica Acta*, 176, pp.1324–1331. <https://doi.org/10.1016/j.electacta.2015.07.151>.

Lalia, B.S., Samad, Y.A. and Hashaikeh, R., 2012. Nanocrystalline-cellulose-reinforced poly(vinylidene fluoride-co- hexafluoropropylene) nanocomposite films as a separator for lithium ion batteries. *Journal of Applied Polymer Science*, 126(SUPPL. 1), pp.E442–E448. <https://doi.org/10.1002/app.36783>.

Lei, Y., Chen, F., Jin, Y. and Liu, Z., 2015. Ag-Cu nanoalloyed film as a high-performance cathode electrocatalytic material for zinc-air battery. *Nanoscale Research Letters*, 10(1). <https://doi.org/10.1186/s11671-015-0900-9>.

Levy, N.R., Lifshits, S., Yohanan, E. and Ein-Eli, Y., 2020. Hybrid Ionic Liquid Propylene Carbonate-Based Electrolytes for Aluminum-Air Batteries. *ACS*

*Applied Energy Materials*, 3(3), pp.2585–2592.  
<https://doi.org/10.1021/acsaem.9b02288>.

Li, Q. and Bjerrum, N.J., 2002. *Aluminum as anode for energy storage and conversion: a review*.

Li, Z., Zhang, D. and Yang, F., 2009. *Developments of lithium-ion batteries and challenges of LiFePO<sub>4</sub> as one promising cathode material*. *Journal of Materials Science*, <https://doi.org/10.1007/s10853-009-3316-z>.

Liang, J., Luo, J., Sun, Q., Yang, X., Li, R. and Sun, X., 2019. *Recent progress on solid-state hybrid electrolytes for solid-state lithium batteries*. *Energy Storage Materials*, <https://doi.org/10.1016/j.ensm.2019.06.021>.

Liu, K., Huang, X., Wang, H., Li, F., Tang, Y., Li, J. and Shao, M., 2016. *Co<sub>3</sub>O<sub>4</sub>-CeO<sub>2</sub>/C as a Highly Active Electrocatalyst for Oxygen Reduction Reaction in Al-Air Batteries*. *ACS Applied Materials and Interfaces*, 8(50), pp.34422–34430. <https://doi.org/10.1021/acsami.6b12294>.

Liu, W., Su, Q., Yu, L., Du, G., Li, C., Zhang, M., Ding, S. and Xu, B., 2021. *Understanding reaction mechanism of oxygen evolution reaction using Ru single atoms as catalyst for Li-O<sub>2</sub> battery*. *Journal of Alloys and Compounds*, 886. <https://doi.org/10.1016/j.jallcom.2021.161189>.

Liu, Y., Sun, Q., Li, W., Adair, K.R., Li, J. and Sun, X., 2017. *A comprehensive review on recent progress in aluminum–air batteries*. *Green Energy and Environment*, <https://doi.org/10.1016/j.gee.2017.06.006>.

Ma, J., Wen, J., Li, Q. and Zhang, Q., 2013. *Effects of acidity and alkalinity on corrosion behaviour of Al-Zn-Mg based anode alloy*. *Journal of Power Sources*, 226, pp.156–161. <https://doi.org/10.1016/j.jpowsour.2012.10.075>.

Maksimov, A. V., Molina, M., Maksimova, O.G. and Gor, G.Y., 2023. Prediction of Swelling of Polypropylene Separators and Its Effect on the Lithium-Ion Battery Performance. *ACS Applied Polymer Materials*, 5(3), pp.2026–2031. <https://doi.org/10.1021/acsapm.2c02074>.

Manthiram, A., 2011. *Materials challenges and opportunities of lithium ion batteries*. *Journal of Physical Chemistry Letters*, <https://doi.org/10.1021/jz1015422>.

Mori, R., 2017a. Electrochemical properties of a rechargeable aluminum-air battery with a metal-organic framework as air cathode material. *RSC Advances*, 7(11), pp.6389–6395. <https://doi.org/10.1039/c6ra25164a>.

Mori, R., 2017b. Rechargeable Aluminum–Air Battery Using Various Air-Cathode Materials and Suppression of Byproducts Formation on Both Anode and Air Cathode. *ECS Transactions*, 80(10), pp.377–393. <https://doi.org/10.1149/08010.0377ecst>.

Mori, R., 2018. Semi-solid-state aluminium-air batteries with electrolytes composed of aluminium chloride hydroxide with various hydrophobic additives. *Physical Chemistry Chemical Physics*, 20(47), pp.29983–29988. <https://doi.org/10.1039/c8cp03997f>.

Mori, R., 2020. *Recent Developments for Aluminum–Air Batteries*. *Electrochemical Energy Reviews*, <https://doi.org/10.1007/s41918-020-00065-4>.

Mussa, A.S., Klett, M., Lindbergh, G. and Lindström, R.W., 2018. Effects of external pressure on the performance and ageing of single-layer lithium-ion pouch cells. *Journal of Power Sources*, 385, pp.18–26. <https://doi.org/10.1016/j.jpowsour.2018.03.020>.

Mutlu, R.N. and Yazıcı, B., 2019. Copper-deposited aluminum anode for aluminum-air battery. *Journal of Solid State Electrochemistry*, 23(2), pp.529–541. <https://doi.org/10.1007/s10008-018-4146-1>.

Olejniak, K., Skalski, B., Stanislawska, A. and Wysocka-Robak, A., 2017. Swelling properties and generation of cellulose fines originating from bleached kraft pulp refined under different operating conditions. *Cellulose*, 24(9), pp.3955–3967. <https://doi.org/10.1007/s10570-017-1404-9>.

Palanisamy, S., Rajendhran, N., Srinivasan, S., Shyma, A.P., Murugan, V., Parasuraman, B. and Kheawhom, S., 2021. A novel nano-YSZ-Al alloy anode for Al–air battery. *Journal of Applied Electrochemistry*, 51(2), pp.345–356. <https://doi.org/10.1007/s10800-020-01493-2>.

Peng, G.S., Huang, J., Gu, Y.C. and Song, G.S., 2020. The Discharge and Corrosion Behavior of Al Anodes with Different Purity in Alkaline Solution. *Int. J. Electrochem. Sci*, [online] 15, pp.6892–6907. <https://doi.org/10.20964/2020.07.59>.

van Ree, T., 2020. *Electrolyte additives for improved lithium-ion battery performance and overcharge protection*. *Current Opinion in Electrochemistry*, <https://doi.org/10.1016/j.coelec.2020.01.001>.

Ren, J., Ma, J., Zhang, J., Fu, C. and Sun, B., 2019. Electrochemical performance of pure Al, Al–Sn, Al–Mg and Al–Mg–Sn anodes for Al-air batteries. *Journal of Alloys and Compounds*, 808. <https://doi.org/10.1016/j.jallcom.2019.151708>.

Rota, M., Comninellis, C., Moller, S., Holzer, F. and Haas, O., 1995. *Bipolar Al/O<sub>2</sub> battery with planar electrodes in alkaline and acidic electrolytes*. *JOURNAL OF APPLIED ELECTROCHEMISTRY*.

Ryu, J., Park, M. and Cho, J., 2019. *Advanced Technologies for High-Energy Aluminum–Air Batteries*. *Advanced Materials*, <https://doi.org/10.1002/adma.201804784>.

Selan, A.A., Saw, L.H., Thiam, H.S., Sun, D. and Tan, W.C., 2023. Preliminary analysis of the cellulose-based battery separator. *Materials Today: Proceedings*. <https://doi.org/10.1016/j.matpr.2023.01.294>.

Shayeb, H.A. El, Abd, F.M., Wahab, E.L., Zein, S. and Abedin, E.L., 1999. *Electrochemical behaviour of Al, Al±Sn, Al±Zn and Al±Zn±Sn alloys in chloride solutions containing indium ions*.

Sun, S., Miao, H., Xue, Y., Wang, Q., Li, S. and Liu, Z., 2016. Oxygen reduction reaction catalysts of manganese oxide decorated by silver nanoparticles for aluminum-air batteries. *Electrochimica Acta*, 214, pp.49–55. <https://doi.org/10.1016/j.electacta.2016.07.127>.

Tan, W.C., Saw, L.H., Yew, M.C., Sun, D., Cai, Z., Chong, W.T. and Kuo, P.Y., 2021. Analysis of the Polypropylene-Based Aluminium-Air Battery. *Frontiers in Energy Research*, 9. <https://doi.org/10.3389/fenrg.2021.599846>.

Tang, Y., Lu, L., Roesky, H.W., Wang, L. and Huang, B., 2004. The effect of zinc on the aluminum anode of the aluminum-air battery. *Journal of Power Sources*, 138(1–2), pp.313–318. <https://doi.org/10.1016/j.jpowsour.2004.06.043>.

Zainuddin, N.K., Saadiah, M.A., Abdul Majeed, A.P.P. and Samsudin, A.S., 2018. Characterization on conduction properties of carboxymethyl cellulose/kappa carrageenan blend-based polymer electrolyte system. *International Journal of Polymer Analysis and Characterization*, 23(4), pp.321–330. <https://doi.org/10.1080/1023666X.2018.1446887>.

Zein El Abedin, S. and Endres, F., 2004. *Electrochemical behaviour of Al, Al-In and Al-Ga-In alloys in chloride solutions containing zinc ions*.

Zein, S., Abedin, E.L. and Saleh, A.O., 2004. *Characterization of some aluminium alloys for application as anodes in alkaline batteries*.

Zhang, J., Yue, L., Kong, Q., Liu, Z., Zhou, X., Zhang, C., Xu, Q., Zhang, B., Ding, G., Qin, B., Duan, Y., Wang, Q., Yao, J., Cui, G. and Chen, L., 2014a. Sustainable, heat-resistant and flame-retardant cellulose-based composite separator for high-performance lithium ion battery. *Scientific Reports*, 4. <https://doi.org/10.1038/srep03935>.

Zhang, L., Huang, Q.A., Yan, W., Shao, Q. and Zhang, J., 2019. Design and fabrication of non-noble metal catalyst-based air-cathodes for metal-air battery. *Canadian Journal of Chemical Engineering*, 97(12), pp.2984–2993. <https://doi.org/10.1002/cjce.23616>.

Zhang, S.S., 2007. *A review on the separators of liquid electrolyte Li-ion batteries.* *Journal of Power Sources*, <https://doi.org/10.1016/j.jpowsour.2006.10.065>.

Zhang, Z., Zuo, C., Liu, Z., Yu, Y., Zuo, Y. and Song, Y., 2014b. All-solid-state Al-air batteries with polymer alkaline gel electrolyte. *Journal of Power Sources*, 251, pp.470–475. <https://doi.org/10.1016/j.jpowsour.2013.11.020>.

Zhao, P., Yang, J., Shang, Y., Wang, L., Fang, M., Wang, J. and He, X., 2015. Surface modification of polyolefin separators for lithium ion batteries to reduce thermal shrinkage without thickness increase. *Journal of Energy Chemistry*, 24(2), pp.138–144. [https://doi.org/10.1016/S2095-4956\(15\)60294-7](https://doi.org/10.1016/S2095-4956(15)60294-7).

Zheng, F., Kotobuki, M., Song, S., Lai, M.O. and Lu, L., 2018. Review on solid electrolytes for all-solid-state lithium-ion batteries. *Journal of Power Sources*, 389, pp.198–213. <https://doi.org/10.1016/j.jpowsour.2018.04.022>.

Zhou, C., Bhonge, K. and Cho, K.T., 2020. Analysis of the effect of hydrogen-evolving side reaction in the aqueous aluminum-air battery. *Electrochimica Acta*, 330. <https://doi.org/10.1016/j.electacta.2019.135290>.



ZHUANG, Z. hang, FENG, Y., PENG, C. qun, YANG, L. zhong and WANG, M., 2021. Effect of Ga on microstructure and electrochemical performance of Al–0.4Mg–0.05Sn–0.03Hg alloy as anode for Al–air batteries. *Transactions of Nonferrous Metals Society of China (English Edition)*, 31(9), pp.2558–2569. [https://doi.org/10.1016/S1003-6326\(21\)65675-3](https://doi.org/10.1016/S1003-6326(21)65675-3).

Aiello, L., Ruchti, P., Vitzthum, S. and Coren, F., 2024. Influence of Pressure, Temperature and Discharge Rate on the Electrical Performances of a Commercial Pouch Li-Ion Battery. *Batteries*, 10(3), p.72. <https://doi.org/10.3390/batteries10030072>.

Etale, A., Onyianta, A. J., Turner, S. R., & Eichhorn, S. J. (2023). Cellulose: A Review of Water Interactions, Applications in Composites, and Water Treatment. In *Chemical Reviews* (Vol. 123, Issue 5, pp. 2016–2048). American Chemical Society. <https://doi.org/10.1021/acs.chemrev.2c00477>

Maksimov, A. V., Molina, M., Maksimova, O. G., & Gor, G. Y. (2023). Prediction of Swelling of Polypropylene Separators and Its Effect on the Lithium-Ion Battery Performance. *ACS Applied Polymer Materials*, 5(3), 2026–2031. <https://doi.org/10.1021/acsapm.2c02074>

Mussa, A. S., Klett, M., Lindbergh, G., & Lindström, R. W. (2018). Effects of external pressure on the performance and ageing of single-layer lithium-ion pouch cells. *Journal of Power Sources*, 385, 18–26. <https://doi.org/10.1016/j.jpowsour.2018.03.020>

Olejniak, K., Skalski, B., Stanislawski, A., & Wysocka-Robak, A. (2017). Swelling properties and generation of cellulose fines originating from bleached kraft pulp refined under different operating conditions. *Cellulose*, 24(9), 3955–3967. <https://doi.org/10.1007/s10570-017-1404-9>